US006315445B1

(12) **United States Patent**
Mazess et al.

(10) **Patent No.: US 6,315,445 B1**
(45) **Date of Patent: Nov. 13, 2001**

(54) **DENSITOMETRY ADAPTER FOR COMPACT X-RAY FLUOROSCOPY MACHINE**

(75) Inventors: **Richard B. Mazess**; **David L. Ergun**; **Joseph P. Bisek**, all of Madison, WI (US)

(73) Assignee: **Lunar Corporation**, Madison, WI (US)

(*) Notice: Subject to any disclaimer, the term of this patent is extended or adjusted under 35 U.S.C. 154(b) by 0 days.

(21) Appl. No.: **09/745,704**

(22) Filed: **Dec. 21, 2000**

Related U.S. Application Data

(62) Division of application No. 09/281,518, filed on Mar. 30, 1999, now Pat. No. 6,215,846, and a continuation-in-part of application No. 09/006,358, filed as application No. PCT/US97/02770 on Feb. 21, 1997, now Pat. No. 6,007,243.

(60) Provisional application No. 60/080,164, filed on Mar. 31, 1998, and provisional application No. 60/011,993, filed on Feb. 21, 1996.

(51) **Int. Cl.**[7] **A61B 6/04**

(52) **U.S. Cl.** **378/196**; 378/55; 378/208

(58) **Field of Search** 378/55, 196, 208

(56) **References Cited**

U.S. PATENT DOCUMENTS

3,639,764	*	2/1972	Olson et al.	378/193
4,829,549		5/1989	Vogel et al.	378/55
5,042,489		8/1991	Wiener et al.	128/661.03
5,136,743	*	8/1992	Pirela-Cruz	5/647
5,336,880		8/1994	Leclerc et al.	250/214
5,416,818		5/1995	Takahashi et al.	378/98.7
5,479,471	*	12/1995	Buckland	378/208
5,748,704	*	5/1998	Mazess et al.	378/54
5,878,108		3/1999	Baba et al.	378/98.4
5,903,008		5/1999	Li	250/363.04
5,905,809		5/1999	Timmer	382/131
5,949,846	*	9/1999	Stein et al.	378/54
6,061,419		5/2000	Hsieh et al.	378/4
6,104,777		8/2000	Darboux et al.	378/62
6,215,846	*	4/2001	Mazess et al.	378/62

* cited by examiner

Primary Examiner—Robert H. Kim
Assistant Examiner—Allen C Ho
(74) *Attorney, Agent, or Firm*—Quarles & Brady LLP

(57) **ABSTRACT**

An accessory for fluoroscopy equipment is provided to support the x-ray tube and detector on a pedestal with respect to a patient limb for quantitative bone densitometry measurement. Software loaded into the associated digital imaging fluoroscopy equipment provides necessary correction of the images for the quantitative accuracy needed for bone densitometry. Alternatively, a specialized detector or extremely low form factor image intensifier may be inserted in the pedestal to be used in lieu of the fluoroscopy equipment detector. A similar software correction is performed on an associated computer when a separate detector must be used.

17 Claims, 13 Drawing Sheets

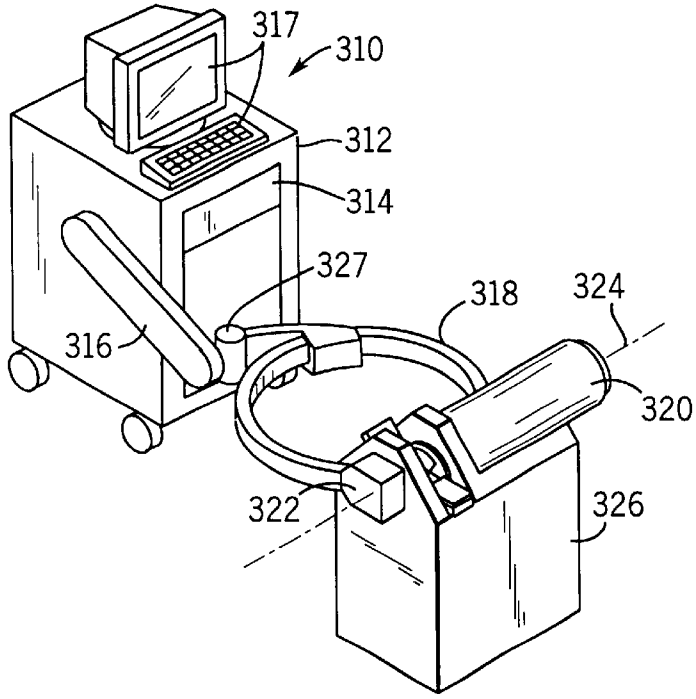

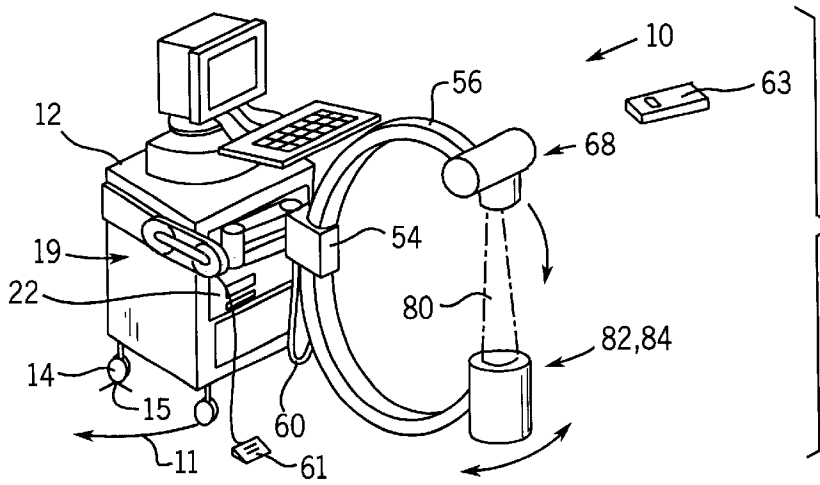

FIG. 1

FIG. 2

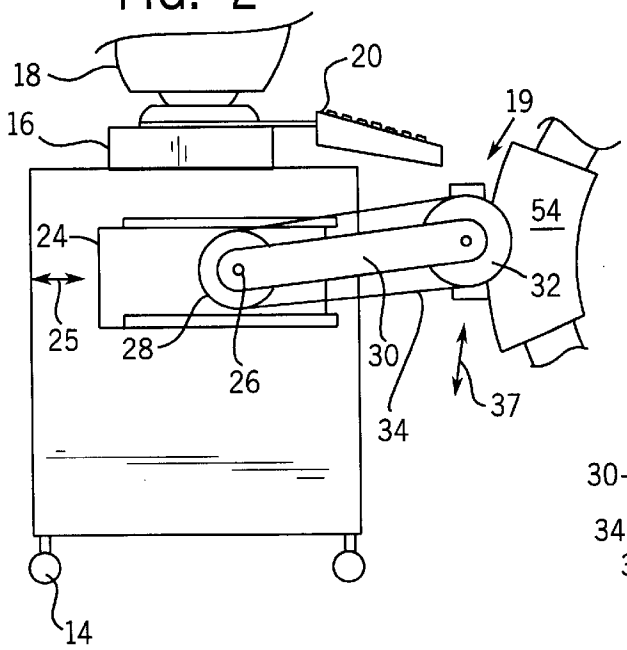

FIG. 3

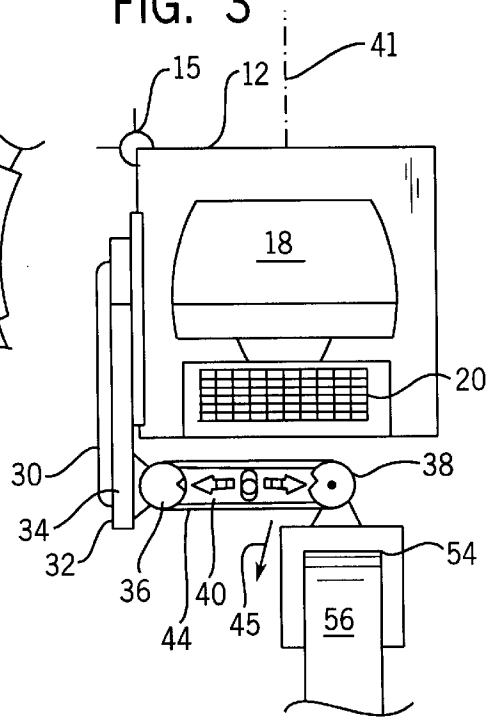

FIG. 4

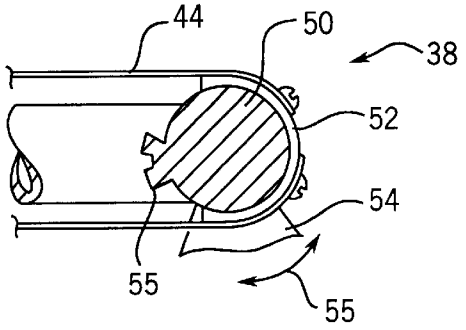

FIG. 5

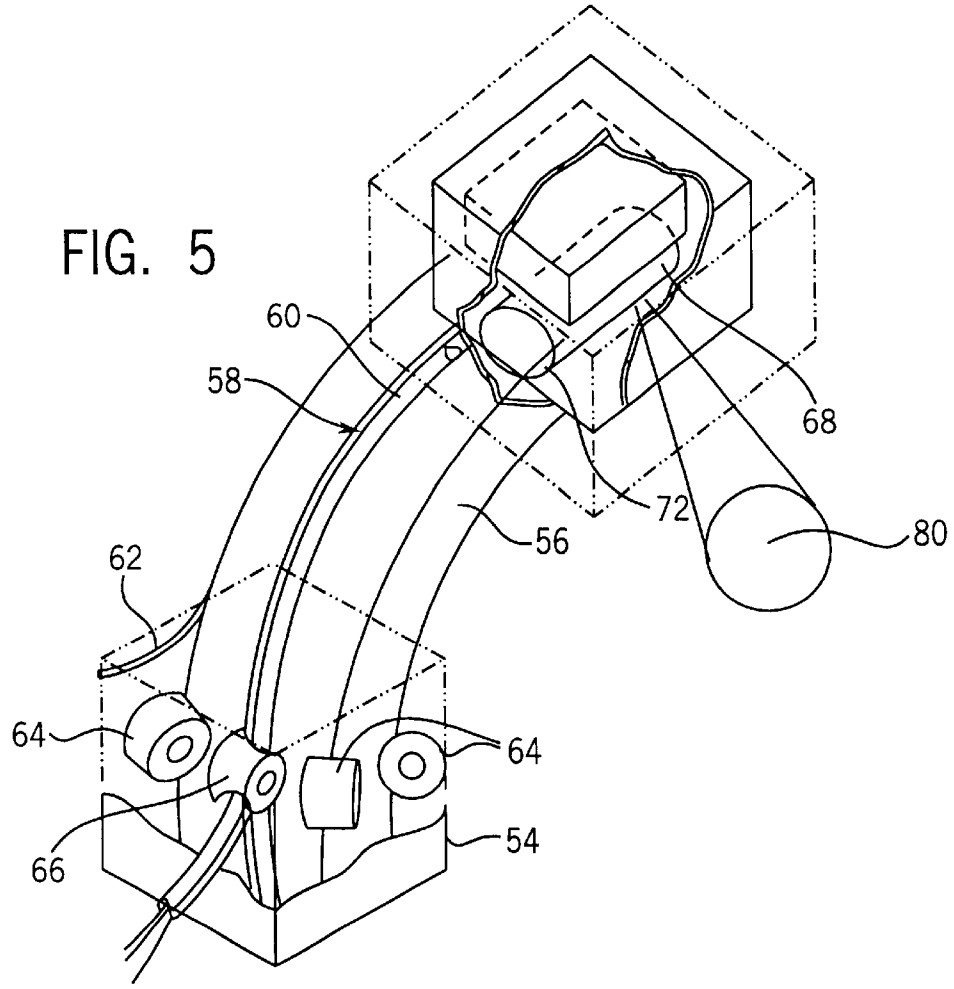
60
58
68
72
56
80
62
64
64
66
54

FIG. 6

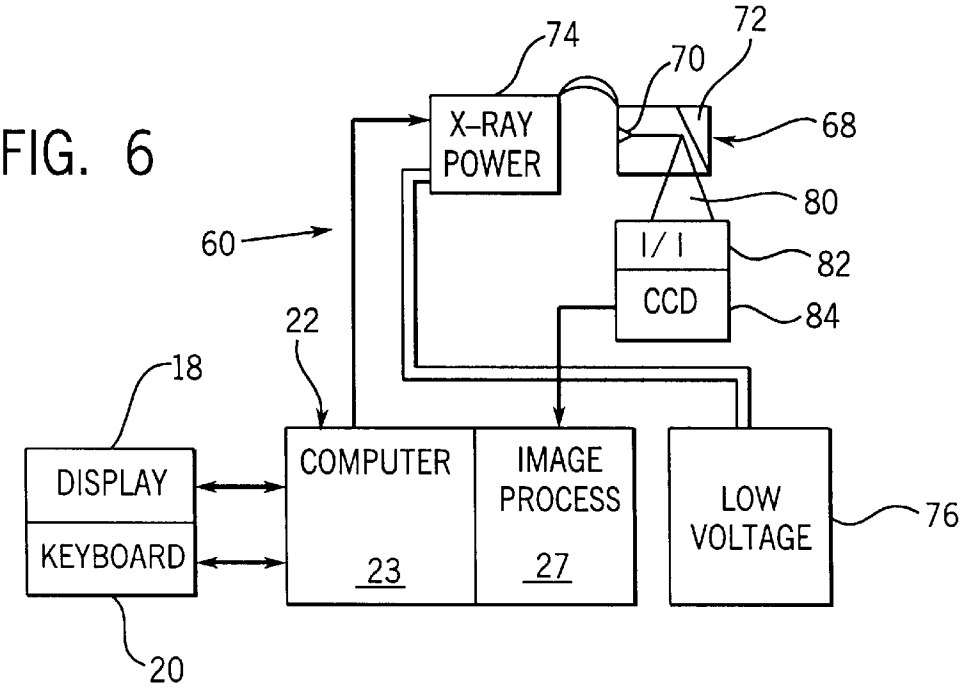
74
72
70
X-RAY POWER
68
80
60
I/I
82
CCD
84
22
18
DISPLAY
KEYBOARD
COMPUTER
23
IMAGE PROCESS
27
LOW VOLTAGE
76
20

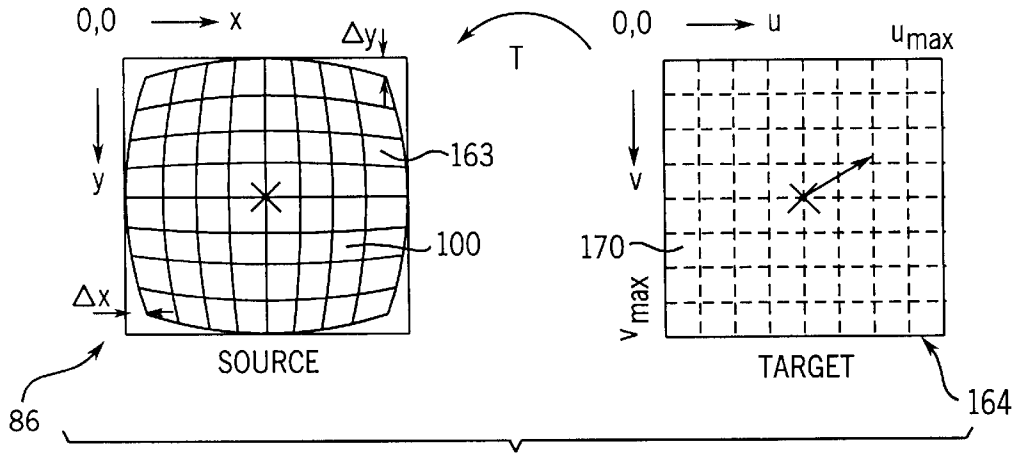

FIG. 19

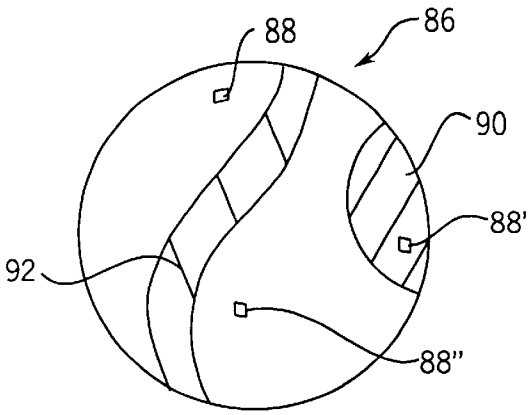

FIG. 7

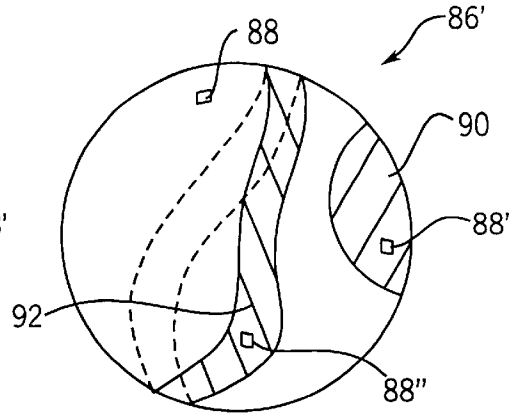

FIG. 8

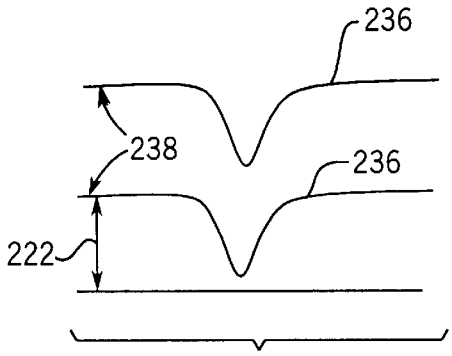

FIG. 24

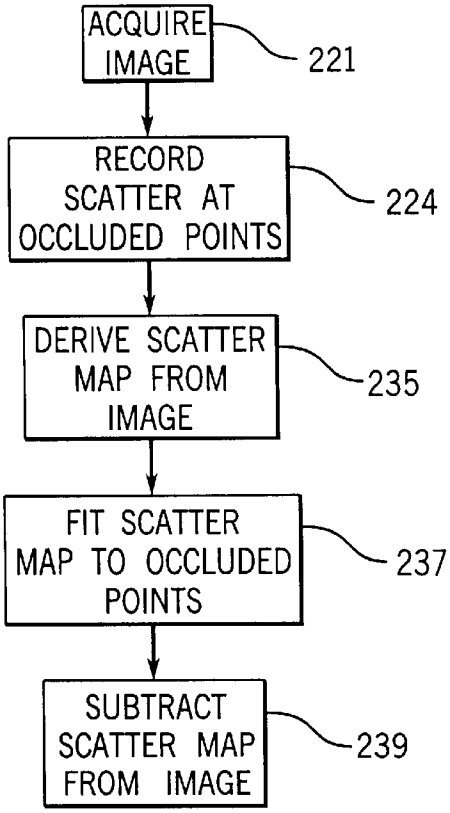
ACQUIRE IMAGE
221
RECORD SCATTER AT OCCLUDED POINTS
224
DERIVE SCATTER MAP FROM IMAGE
235
FIT SCATTER MAP TO OCCLUDED POINTS
237
SUBTRACT SCATTER MAP FROM IMAGE
239

FIG. 22

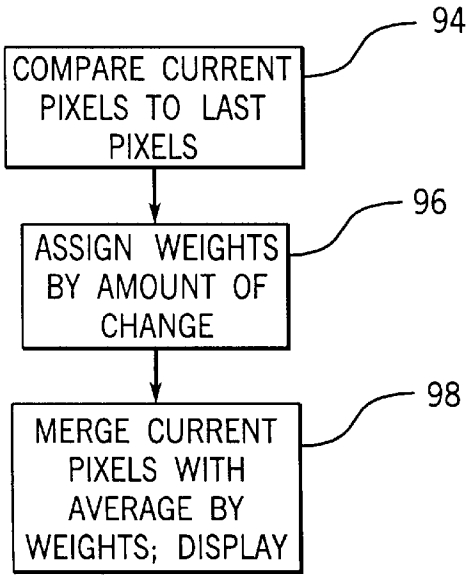
94
COMPARE CURRENT PIXELS TO LAST PIXELS
96
ASSIGN WEIGHTS BY AMOUNT OF CHANGE
98
MERGE CURRENT PIXELS WITH AVERAGE BY WEIGHTS; DISPLAY

FIG. 9

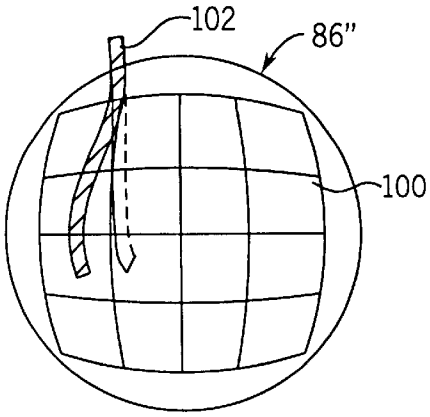

FIG. 10

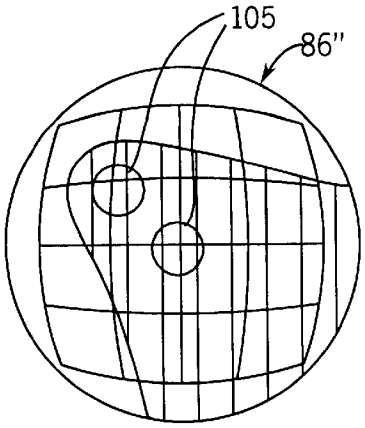

FIG. 11

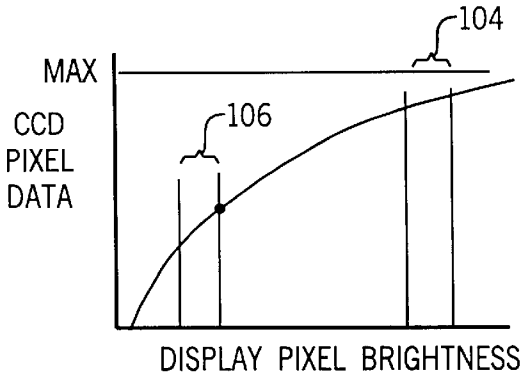

FIG. 12

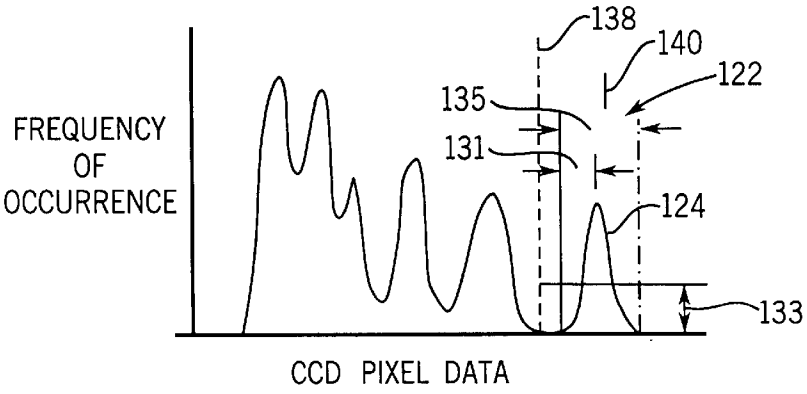

FIG. 13

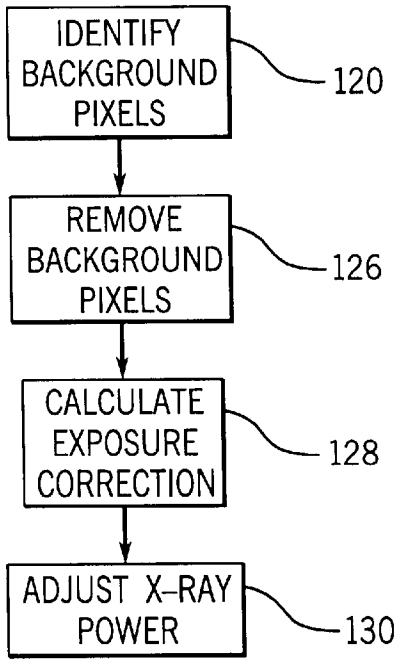
IDENTIFY BACKGROUND PIXELS
120
REMOVE BACKGROUND PIXELS
126
CALCULATE EXPOSURE CORRECTION
128
ADJUST X-RAY POWER
130

FIG. 14

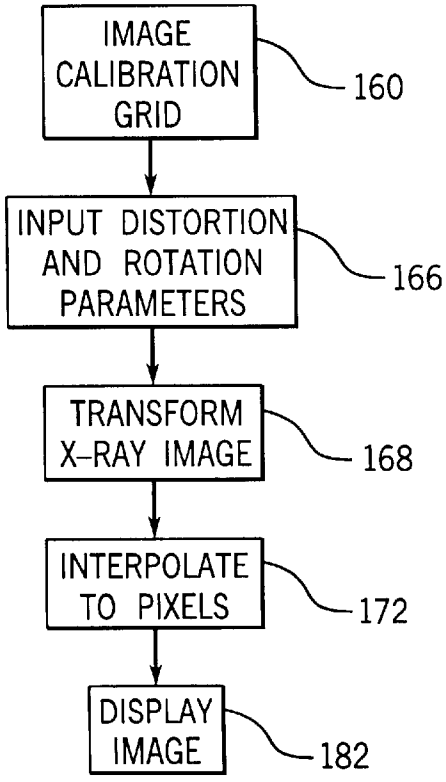
IMAGE CALIBRATION GRID
160
INPUT DISTORTION AND ROTATION PARAMETERS
166
TRANSFORM X-RAY IMAGE
168
INTERPOLATE TO PIXELS
172
DISPLAY IMAGE
182

FIG. 20

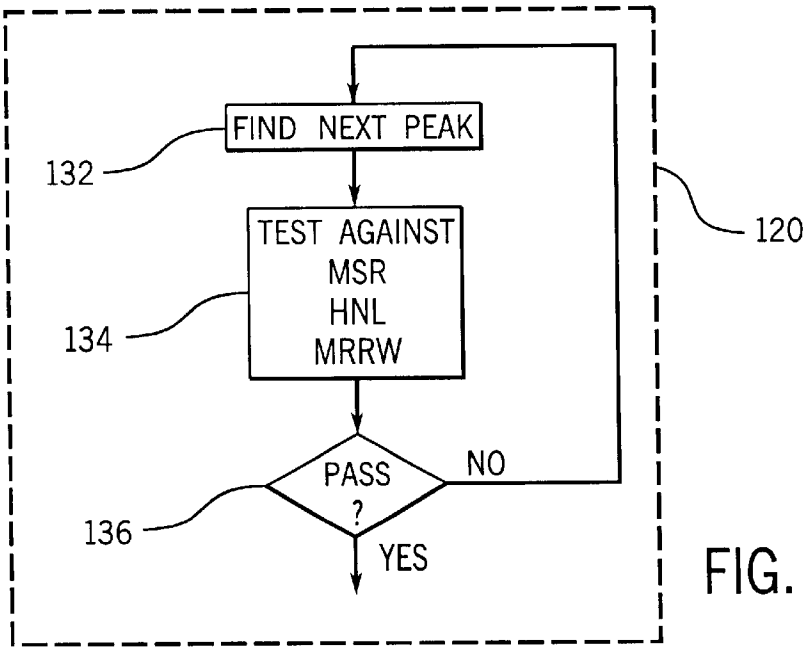

FIG. 15

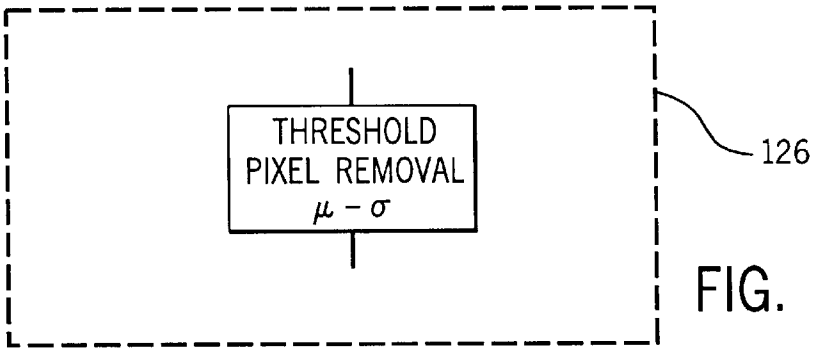

FIG. 16

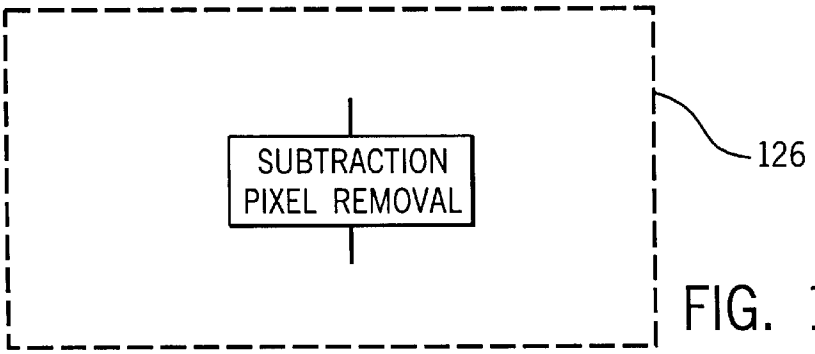

FIG. 17

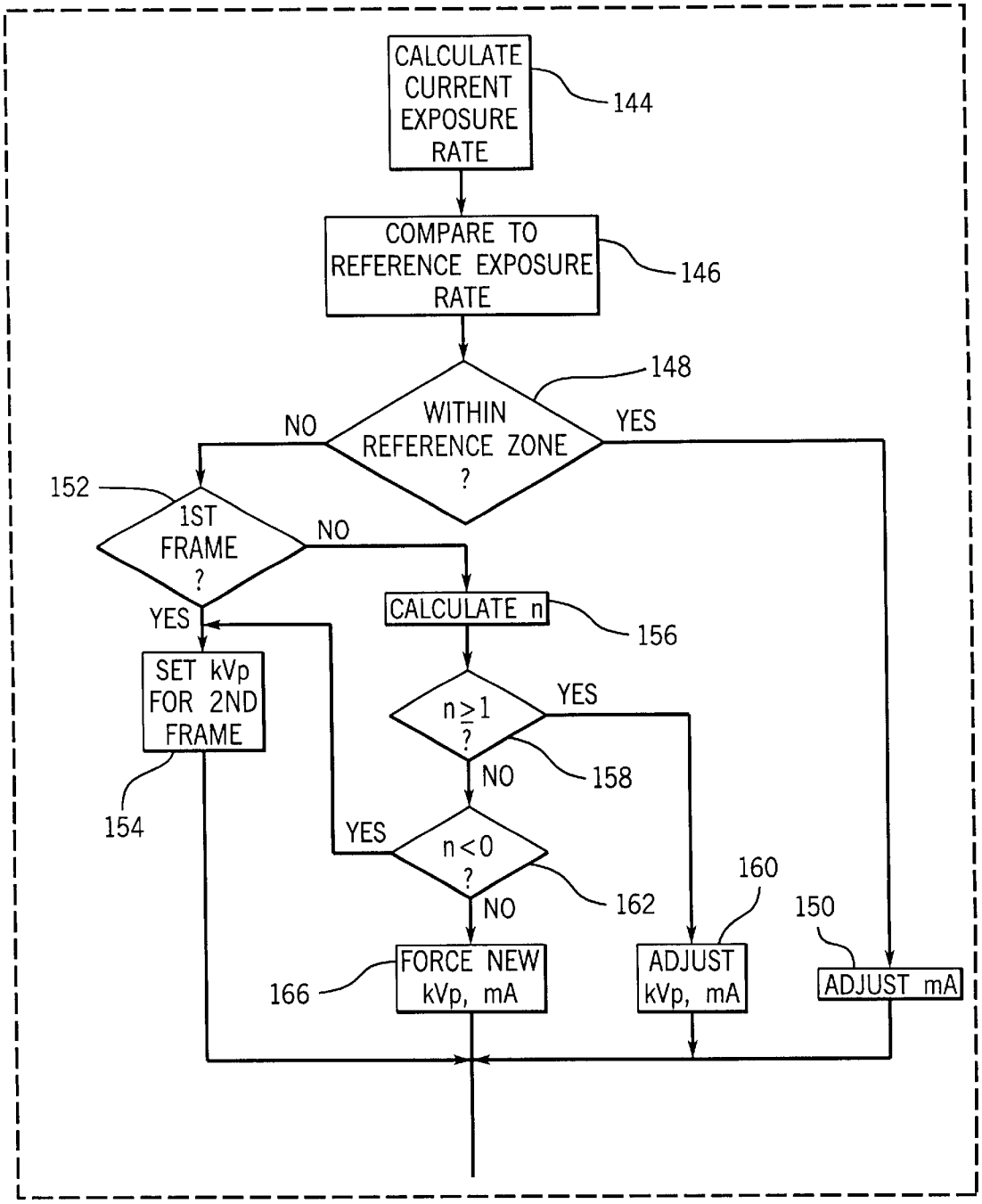
CALCULATE CURRENT EXPOSURE RATE
144
COMPARE TO REFERENCE EXPOSURE RATE
146
148
WITHIN REFERENCE ZONE ?
NO
YES
152
1ST FRAME ?
NO
YES
CALCULATE n
156
SET kVp FOR 2ND FRAME
154
n≥1 ?
YES
158
NO
YES
n<0 ?
162
NO
160
150
FORCE NEW kVp, mA
166
ADJUST kVp, mA
ADJUST mA

FIG. 18

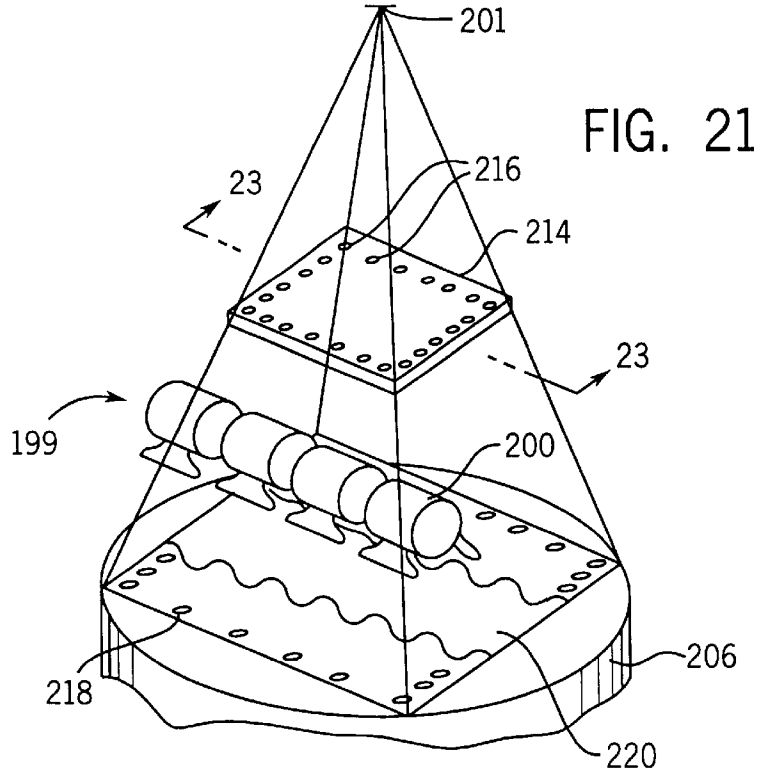
201
216
214
23
23
199
200
206
218
220

FIG. 21

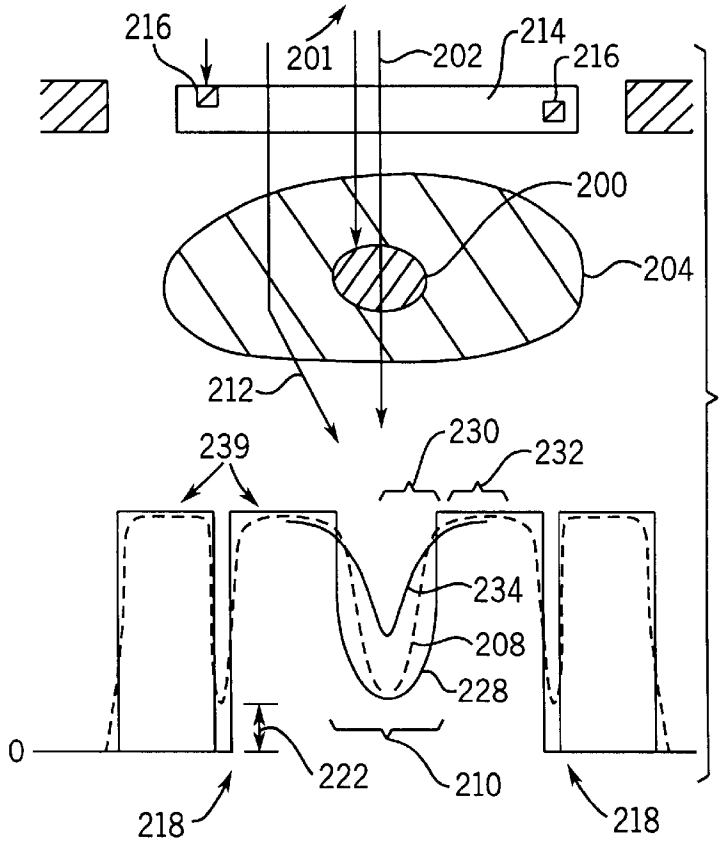
216
201
202
214
216
200
204
212
239
230
232
234
208
228
0
222
210
218
218

FIG. 23

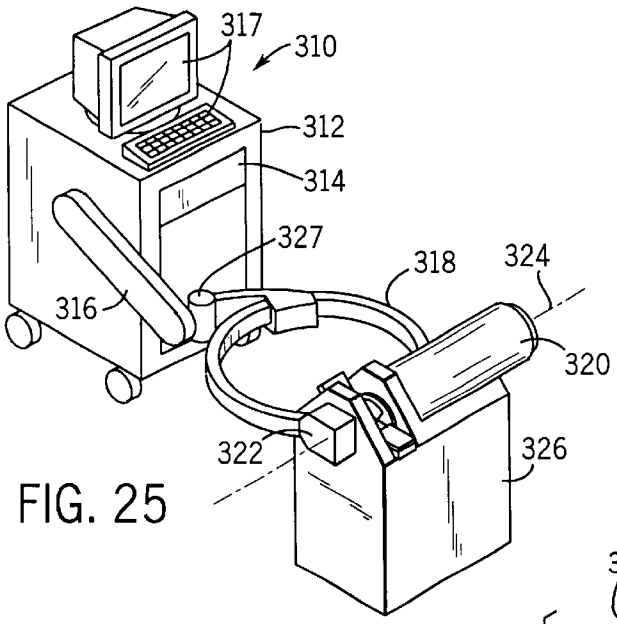

FIG. 25

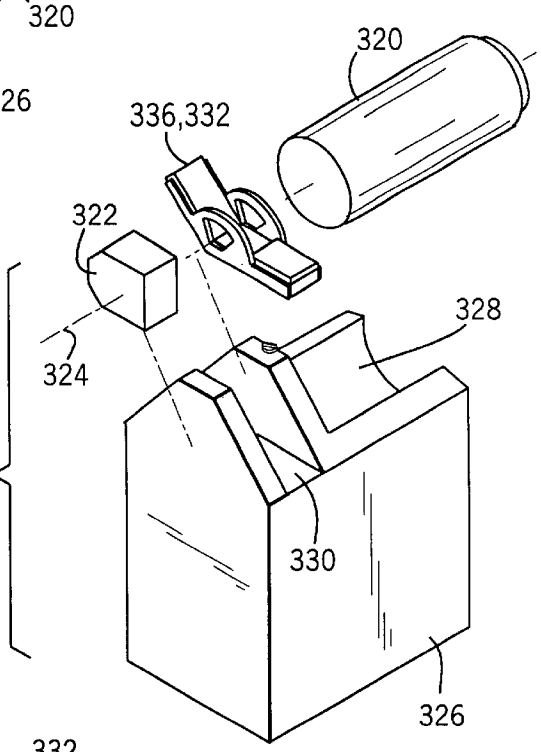

FIG. 26

FIG. 27

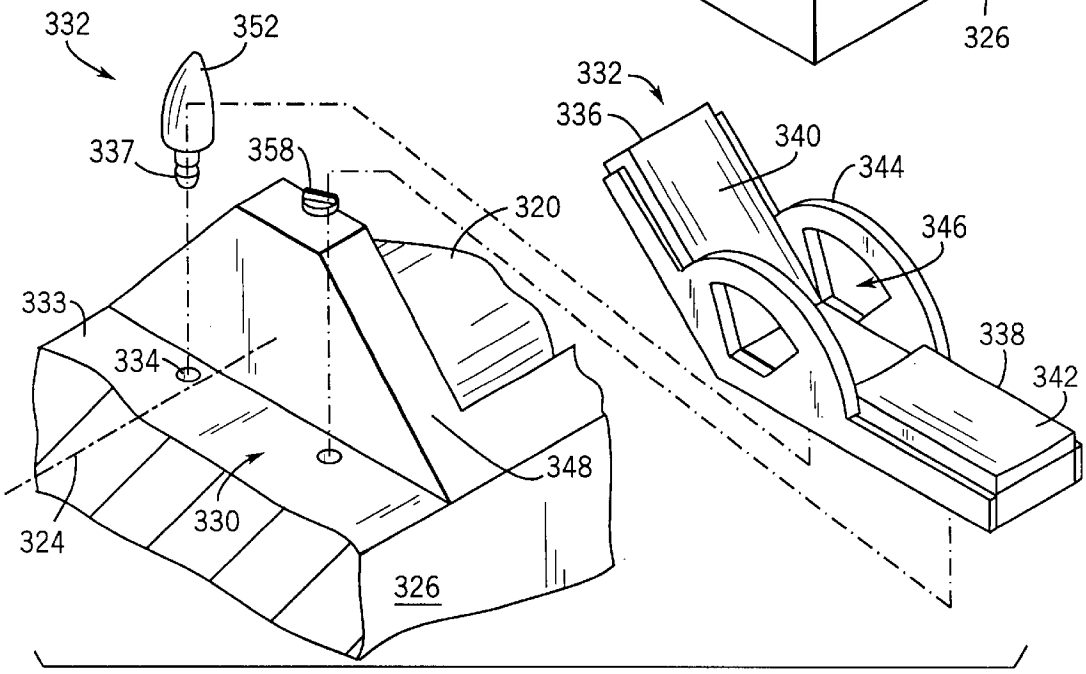

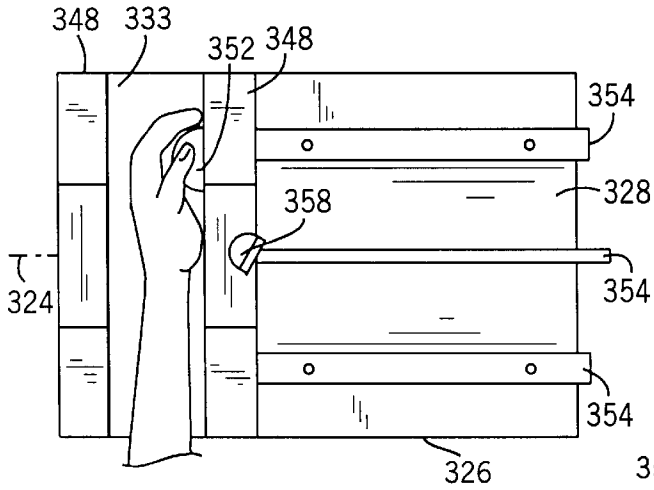

FIG. 28

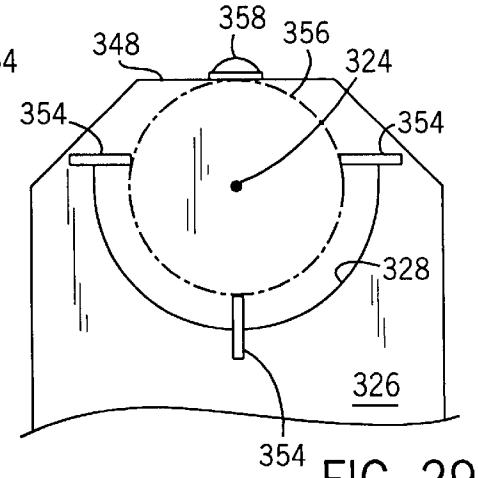

FIG. 29

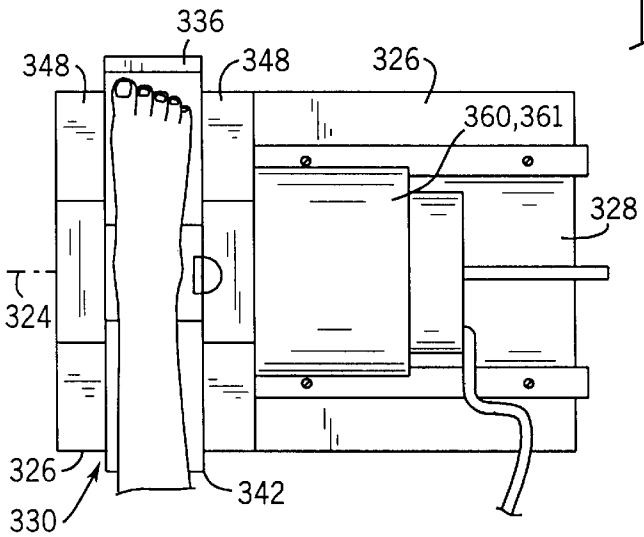

FIG. 30

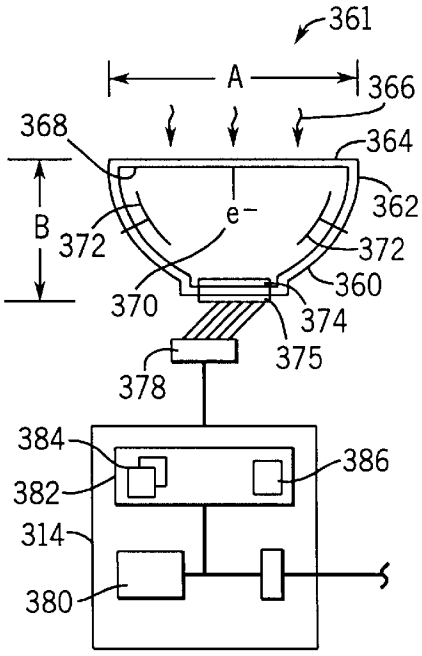

FIG. 31

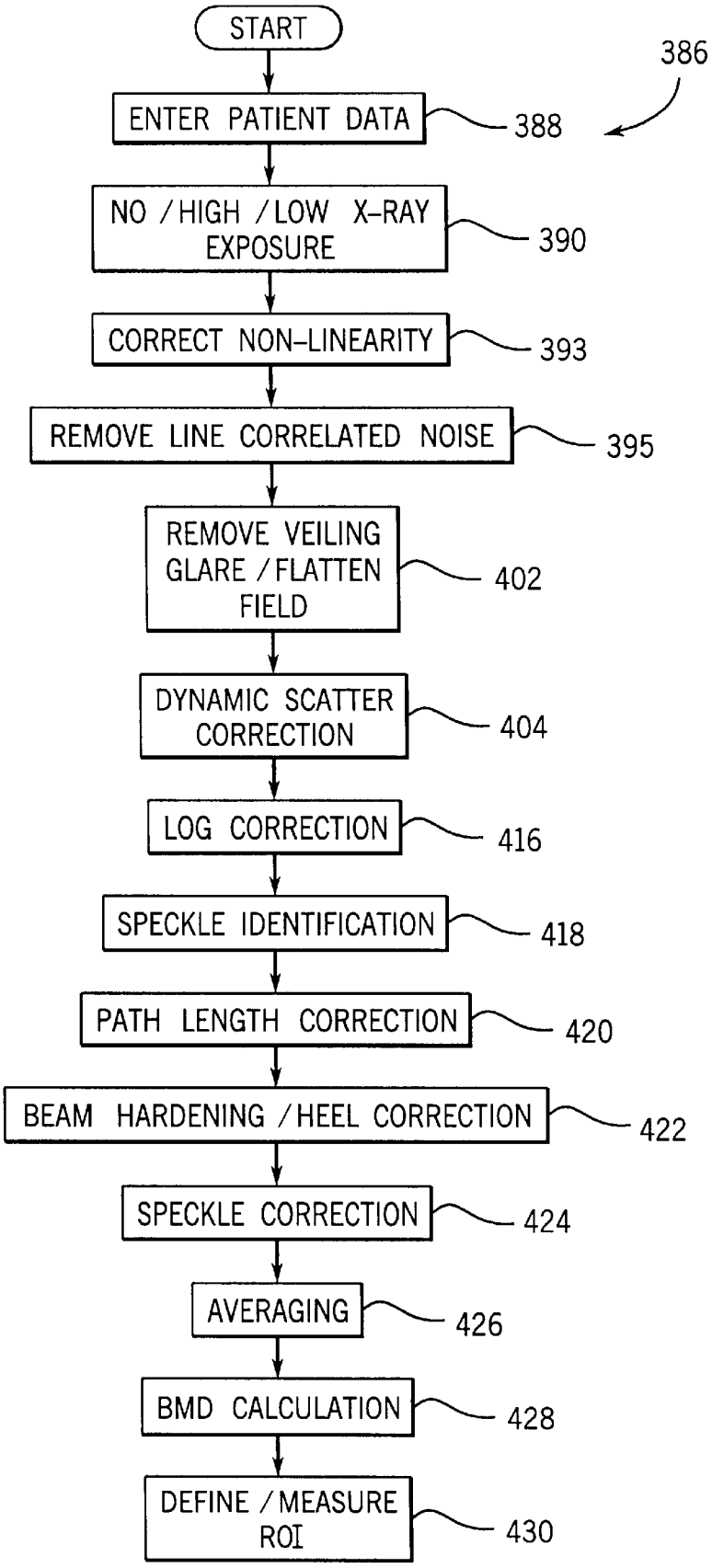
START
386
ENTER PATIENT DATA
388
NO / HIGH / LOW X-RAY EXPOSURE
390
CORRECT NON-LINEARITY
393
REMOVE LINE CORRELATED NOISE
395
REMOVE VEILING GLARE / FLATTEN FIELD
402
DYNAMIC SCATTER CORRECTION
404
LOG CORRECTION
416
SPECKLE IDENTIFICATION
418
PATH LENGTH CORRECTION
420
BEAM HARDENING / HEEL CORRECTION
422
SPECKLE CORRECTION
424
AVERAGING
426
BMD CALCULATION
428
DEFINE / MEASURE ROI
430

FIG. 32

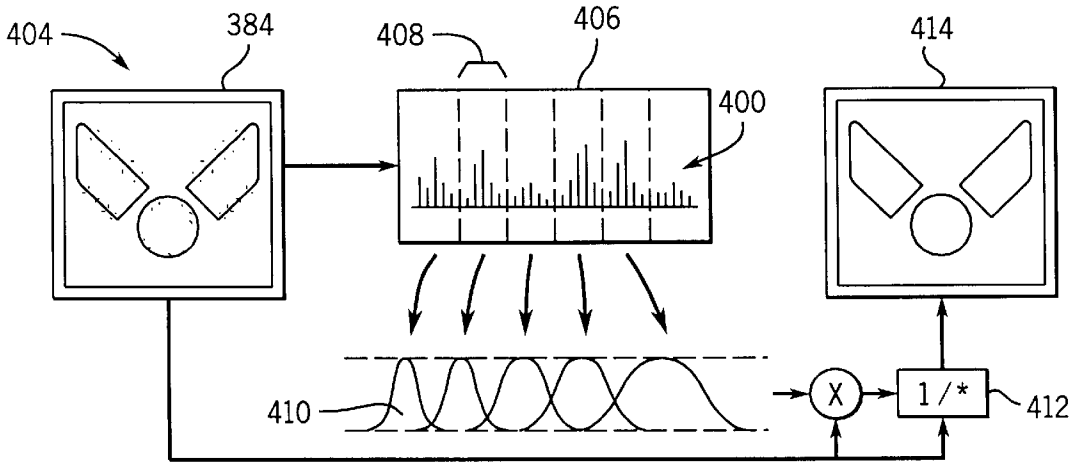

FIG. 33

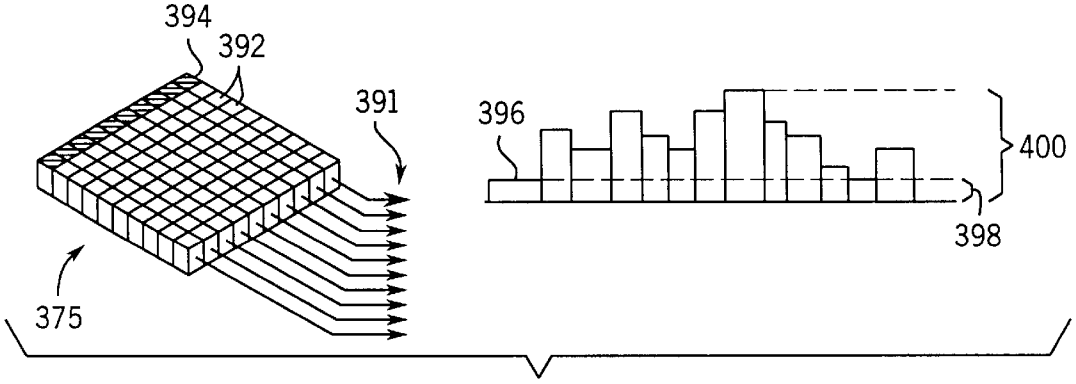

FIG. 34

DENSITOMETRY ADAPTER FOR COMPACT X-RAY FLUOROSCOPY MACHINE

CROSS-REFERENCE TO RELATED APPLICATIONS

This application is a divisional of U.S. application Ser. No. 09/281,518 filed Mar. 30, 1999, U.S. Pat. No. 6,215,846, which is based on U.S. provisional application no. 60/080,164 filed Mar. 31, 1998 and is a continuation in part of U.S. application Ser. No. 09/006,358 filed Jan. 13, 1998, U.S. Pat. No. 6,007,243, which is a continuation in part of PCT application US Ser. No. 97/02770 designating the United States filed Feb. 21, 1997 claiming benefit of provisional application no. 60/011,993 filed Feb. 21, 1996. This provisional application is incorporated by reference herein.

STATEMENT REGARDING FEDERALLY SPONSORED RESEARCH OR DEVELOPMENT

FIELD OF THE INVENTION

The invention relates generally to x-ray equipment and in particular to an adapter for bone density measurements as may be used with compact x-ray fluoroscopy equipment used for orthopedic and similar procedures.

BACKGROUND OF THE INVENTION

Portable x-ray fluoroscopy machines provide an x-ray source held in opposition to an electronic image detector, typically on a C-arm, so that x-rays from the x-ray source are received by the image detector. The C-arm may slide through a collar so as to allow it to be rotated to different angles about the patient. Further, the collar may be supported by a pivoting arm providing additional freedom in the positioning of the C-arm.

When the C-arm is correctly positioned, the x-ray source is activated and x-rays pass through the patient to be received by the image detector which provides electronic signals to a video monitor. For larger mobile C-arm systems, the video monitor is typically held on a separate cart or may be suspended from the ceiling on a fixed bracket to be connected to the mobile unit when the mobile unit is in place.

With improvements in electronic hardware and in particular the development of compact image intensifiers and CCD video cameras, it has become possible to build extremely compact mobile C-arm systems. Such systems may make use of increasingly powerful desktop computer technology for image processing and other tasks and may use compact digital printers for producing images.

BRIEF SUMMARY OF THE INVENTION

The present invention provides an adapter that may convert a compact fluoroscopy machine or other mobile x-ray source into a precision quantitative densitometer suitable for measuring bone mass or density such as may be helpful in the treatment and detection of osteoporosis.

The invention provides a stand to be used with a fluoroscopy machine, the stand having a cradle for accurately locating the x-ray source and/or detector with respect to either the patient's forearm or foot. Special software is loaded to the computer of the fluoroscopy machine to operate the fluoroscopy machine in a quantitative dual energy mode and to adapt the fluoroscopy data to densiometric data. For fluoroscopy equipment not providing for digital imaging or that may not be easily operated in a dual energy mode, the invention includes a provision for a separate digital dual energy detector and if necessary an associated processing computer.

Other objects, advantages, and features of the present invention will become apparent from the following specification when taken in conjunction with the accompanying drawings.

BRIEF DESCRIPTION OF THE SEVERAL VIEWS OF THE DRAWINGS

FIG. **1** is a perspective view of the fluoroscopy machine suitable for use with the present invention showing a C-arm supporting an image intensifier/video camera and x-ray tube in opposition for rotation in a vertical plane, the C-arm held along a mid-line of a cart by an articulated arm attached to the side of the cart;

FIG. **2** is a side view in elevation of the cart of FIG. **1** showing a slide attaching the articulated arm to the side of the cart and showing a four-bar linkage motion of the arm for elevation of the C-arm;

FIG. **3** is a top view of the C-arm system of FIG. **1** with the articulated arm in partial phantom showing the four-bar linkage of the arm for extending the C-arm toward and away from the cart;

FIG. **4** is a detail fragmentary view of an outer pivot of the articulated arm attached to the C-arm such as allows limited pivoting of a plane of rotation of the C-arm about a vertical axis;

FIG. **5** is a detail view of the C-arm of FIG. **1** and the attached x-ray tube assembly showing the electrical cabling providing power to an x-ray tube power supply fitting into a groove in the C-arm and showing an abutment of the anode of the x-ray tube against the metal casting of the C-arm for heat sinking purposes;

FIG. **6** is a schematic block diagram of the fluoroscopy machine of FIG. **1** showing the path of control of a remote x-ray tube power supply by a microprocessor and the receipt of data from the image intensifier/video camera by the microprocessor for image processing;

FIGS. **7** and **8** are simplified images such as may be obtained by the system of FIG. **1** showing portions of the image having moving elements and portions having stationary elements;

FIG. **9** is a flow chart of a method of the present invention providing differently weighted noise reduction to different areas of the image based on motion in the areas of the image;

FIG. **10** is a figure similar to that of FIG. **7** showing an image of a rectilinear grid as affected by pincushion distortion in the image intensifier and video camera optics such as may provide a confusing image of a surgical tool being manipulated in real-time;

FIG. **11** is a figure similar to FIG. **10** showing equal areas of the image that encompass different areas of the imaged object, such variation as may affect quantitative bone density readings;

FIG. **12** is a plot of raw image data from the image intensifier/video camera as is translated into pixel brightness in the images of FIGS. **7**, **8**, **10**, and **11** by the microprocessor of FIG. **6** according to a non-linear mapping process such as provides noise equilibrium in the images and maximum dynamic range for clinical data;

FIG. **13** is a histogram plotting values of data from the image intensifier/video camera versus the frequency of occurrence of data values showing an isolated Gaussian distribution at the right most side representing unattenuated x-ray values;

FIG. **14** is a flowchart describing the steps taken by the programmed microprocessor of FIG. **6** to identify background pixels and remove them from a calculation of exposure rate used for controlling the remote x-ray tube power supply of FIG. **6**;

FIG. **15** is a detailed block diagram of the first block of the flow chart of FIG. **14**;

FIG. **16** is a first embodiment of the second block of the flow chart of FIG. **14**;

FIG. **17** is a second embodiment of the second block of the flow chart of FIG. **14**;

FIG. **18** is a detailed flow chart of the third block of the flow chart of FIG. **14**;

FIG. **19** is a schematic representation of a distorted image of FIG. **11** and a schematic representation of a corresponding undistorted image showing the variables used in the mathematical transformation of the distorted image to correct for rotation and distortion;

FIG. **20** is a flow chart of the steps performed by the computer in correcting and transforming the image of FIGS. **11** and **19**;

FIG. **21** is a perspective view of an occluder placed in an x-ray beam prior to an imaged object and used for calculating scatter;

FIG. **22** is a flow chart of the steps of calculating and removing scatter using the occluder of FIG. **21**;

FIG. **23** is a cross-sectional view through the occluder of an imaged object of FIG. **21** along line **23**—**23**, aligned with a graph depicting attenuation of x-rays as a function distance along the line of cross-section as well as theoretical attenuation without scatter and scatter components;

FIG. **24** is a graphical representation of an adjustment of calculated scatter from the image of FIG. **23** based on normalizing points established by the occluder of FIG. **21**;

FIG. **25** is a perspective view similar to that of FIG. **1** showing a C-arm system similar to that of FIG. **1** in position on the densitometry cradle of the present invention to provide a beam of x-rays along a horizontal axis across the top of the cradle;

FIG. **26** is a fragmentary exploded view of the x-ray detector and x-ray source of the C-arm system of FIG. **25** removed from the cradle and showing a removable foot positioner also removed from the cradle;

FIG. **27** is an enlarged, fragmentary view of FIG. **26** showing the alternative fitting of a forearm positioner or the foot positioner within a channel of the cradle along the path of x-rays between the x-ray source and x-ray detector;

FIG. **28** is a top plan view of the cradle of FIG. **25** but with the C-arm removed, showing the forearm positioner in use with a patient's arm;

FIG. **29** is a side elevational view of the cradle of FIG. **28**;

FIG. **30** is a top plan view of the cradle of FIG. **28** but with the foot positioner in use with a patient's leg and showing the use of an auxiliary pancake image intensifier for use with fluoroscopy or other x-ray equipment not having suitable dual energy or digital imaging capabilities;

FIG. **31** is a cross sectional view of the pancake image intensifier of FIG. **30** with the protective shrouding removed and taken along a plane including the x-ray beam axis showing the compact, high distortion configuration and an attached processing computer;

FIG. **32** is a flow chart of software executed by a processing computer associated with the x-ray detector for providing quantitative densiometric data;

FIG. **33** is a block diagram of the steps of scatter correction of the present invention; and

FIG. **34** is a block diagram illustrating the removal of line correlated noise per the present invention.

DETAILED DESCRIPTION OF THE INVENTION

C-arm Support Mechanism

Referring now to FIG. **1**, an x-ray machine **10** per the present invention includes a generally box-shaped cart **12** having castors **14** extending downward from its four lower corners. The castors **14** have wheels rotating about a generally horizontal axis, and swiveling about a generally vertical axis passing along the edges of the cart **12**. Castors **14**, as are understood in the art, may be locked against swiveling and/or against rotation.

With one castor **14** locked and the others free to rotate and swivel, a pivot point **15** for the cart **12** is established with respect to the floor such as may be used as a first positioning axis **11** for the x-ray machine **10**.

Positioned on the top of the cart **12** is a turntable **16** holding a video monitor **18** and attached keyboard **20** for swiveling about a vertical axis for convenience of the user. The video monitor **18** and the keyboard **20** may swivel separately so that one operator may view the video monitor **18** while a second operates the keyboard **20**.

The video monitor **18** and the keyboard **20** allow for control of a computer **22** contained in a shelf on the cart **12** open from the front of the cart **12**. The computer **22** may include a general microprocessor-type processor **23** and a specialized image processor **27** for particular functions as will be described. The computer **22** further includes a number of interface boards allowing it to provide control signals to various components of the x-ray machine **10** as will be described and to receive x-ray image data. In addition, the computer **22** receives signals from a foot switch **61** that is used to activate the x-ray system for a brief exposure. Control of the computer **22** may also be accomplished through a remote control wand **63** of a type known in the art.

Referring now also to FIG. **2**, attached to the right side of the cart **12** is a horizontal slide **24** positioned to provide an attachment point **26** for an articulated arm **19** supporting a substantially circular C-arm **56**, which in turn holds an x-ray tube **68** and an image intensifier **82** and camera **84**, in opposition, and facing each other as will be described below. The function of the x-ray tube, the image intensifier and the camera are well known in the prior art in the use of mobile C-arm type x-ray devices used for image display and are described in U.S. Pat. No. 4,797,907 hereby incorporated by reference as part of the prior art. The C-arm may be mass balanced, that is to say its weight may be distributed to reduce its tendency to rotate through collar **54** so that minimal frictional pressure may be used to prevent it from moving.

The articulated arm **19** may be slid horizontally toward the front of the cart **12** to provide a second positioning axis **25** of the x-ray machine **10**. A first pulley **28** is rotatively fixed in a vertical plane, attached to the portion of the slide **24** that may move with respect to the cart **12**, and is pivotally attached to a rigid arm **30** extending toward the front of the cart **12**. The other end of the rigid arm **30** supporting a second pulley **32** is also mounted to swivel with respect to arm **30**. A belt **34** wraps around a portion of the circumference of each of pulleys **28** and **32** and is affixed at one point

along that circumference to each of the pulleys **28** and **32** so that pivoting motion of the arm **30** about the center point **26** of pulley **28** causes rotation of pulley **32** so that it maintains a fixed rotational orientation with respect to the cart **12** as pulley **32** and hence C-arm **56** is moved up and down along a third axis **37**. The linkage, so created, is a variation of the "four bar linkage" well known in the art.

Helical tension springs (not shown for clarity) balance the pulley **32** in rotative equilibrium about point **26** against the weight of the articulated arm **19**, C-arm **56**, and other devices attached to the arm **19**.

Attached to pulley **32** is a third pulley **36** extending in a generally horizontal plane perpendicular to the plane of pulley **32**. The third pulley **32** is attached pivotally to a second rigid arm **40** which at its other end holds another pulley **38** positioned approximately at the midline **41** of the cart **12**. The midline **41** symmetrically divides the left and right sides of the cart **12**.

Portions of the circumference of pulleys **36** and **38** are also connected together by a belt **44** so as to form a second four bar linkage allowing pulley **38** to move toward and away from the cart **12**, along a fourth positioning axis **45**, with pulley **38** and C-arm **56** maintaining their rotational orientation with respect to cart **12**.

Referring now to FIG. **4**, pulley **38** includes a center shaft member **50** having a coaxial outer collar **52** to which belt **44** is attached. A stop **55** attached to the shaft **50** limits the motion of the collar **52** in rotation with respect to the shaft **50** to approximately 26 degrees. Frictional forces between shaft **50** and collar **52** cause shaft **50** to maintain its rotational orientation with respect to collar **52** and hence with respect to pulley **36** until sufficient force is exerted on shaft **50** to displace it with respect to collar **52**. Thus pressure on the C-arm **56** can provide some pivoting motion of the C-arm about the axis of the pulley along the fifth positional axis **55**.

Referring now to FIGS. **1**, **3** and **4**, attached to the shaft **50** is a C-arm collar **52** supporting the arcuate C-arm **56** curving through an approximately 180 degree arc in a vertical plane substantially aligned with the midline **41** of the cart **12** as has been mentioned. The shaft **50** may connect to collar **52** so that the latter may swivel in about a horizontal axis bisecting the circle of the C-arm **56**. This axis may be aligned with the center of mass of the C-arm **56** so that there is not a self-righting tendency of the C-arm or the axis may be placed above the axis of the C-arm so as to provide for a beneficial self righting action. This motion is orthogonal to that provided by motion of shaft **50** and may augment that provided by the castors **14**. Techniques of balancing the C-arm in its various rotational modes, when this is desired, is taught by U.S. Pat. No. 5,038,371 to Janssen issued Aug. 6th, 1991 and hereby incorporated by reference as exemplifying the known prior art understood to all those of ordinary skill in the art.

As described above, motion of the collar **52** may be had in a vertical manner by means of the parallelogram linkage formed by pulleys **28** and **32** of the articulated arm **19** as shown in FIG. **2**. Forward and backward motion away from and toward the cart **12** may be had by the second four bar linkage formed from pulleys **36** and **38**. A slight pivoting of the C-arm **56** about a vertical axis slightly to the rear of the collar **52** and concentric with the axis of pulley **38** may be had by means of the rotation between collar **52** and **50** of FIG. **4**. Greater rotation of the C-arm about the vertical axis passing through pivot point **15** may be had by rotation of the cart about one of its stationary castors **14**. Thus, considerable flexibility in positioning the C-arm may be had.

Referring now to FIG. **5**, the C-arm **56** is an aluminum casting having formed along its outer circumference a channel **58** into which a cable **60** may be run as will be described. C-arm **56** has a generally rectangular cross-section taken along a line of radius of the C-arm arc. Each corner of that rectangular cross-section holds a hardened steel wire **62** to provide a contact point for corner bearings **64** within the collar **52**. The corner bearings **64** support the C-arm **56** but allow movement of the C-arm **56** along its arc through the collar **52**.

A cable guide pulley **66** positioned over the channel **58** and having a concave circumference feeds the cable **60** into the channel **58** as the C-arm moves preventing tangling of the cable **60** or its exposure at the upper edge of the C-arm **56** when the C-arm **56** is rotated. The excess length of cable **60** loops out beneath the collar **52**.

X-Ray Tube Cooling

Referring now to FIGS. **5** and **6**, the C-arm supports at one end a generally cylindrical x-ray tube **68** having a cathode **70** emitting a stream of electrons against a fixed anode **72**. The conversion efficiencies of x-ray tubes are such that the anode **72** can become quite hot and typically requires cooling. In the present invention, the anode **72** is positioned to be bolted against the aluminum casting of the C-arm **56** thereby dissipating its heat into a large conductive metal structure of the C-arm **56**.

The x-ray tube **68** is connected to an x-ray tube power supply **74** which separately controls the current and voltage to the x-ray tube **68** based on signals received from the computer **22** as will be described. The control signals to the x-ray tube power supply **74** are encoded on a fiber optic within the cable **60** to be noise immune. Low voltage conductors are also contained within cable **60** to provide power to the x-ray tube power supply **74** from a low voltage power supply **76** positioned on the cart **12**.

During operation, an x-ray beam **80** emitted from the x-ray tube **68** passes through a patient (not shown) and is received by an image intensifier **82** and recorded by a charge couple device ("CCD") camera **84** such as is well known in the art. The camera provides digital radiation values to the computer **22** inversely proportional to the x-ray absorption of the imaged object for processing as will be described below. Each radiation value is dependent on the intensity of x-ray radiation received at a specific point on the imaging surface of the image intensifier **82**.

Image Noise Reduction

Referring now to FIGS. **6** and **7**, the data collected by the CCD camera **84** may be used to provide an image **86** displayed on video monitor **18**. As will be described in more detail below, the CCD camera receiving a light image from the image intensifier **82** at a variety of points, provides data to the computer which maps the data from the CCD camera **84** to a pixel **88** in the image **86**. For convenience, the data from the CCD camera **84** will also be termed radiation data reflecting the fact that there is not necessarily a one-to-one correspondence between data detected by the CCD camera **84** and pixels **88** displayed on the video monitor **18**.

The CCD camera **84** provides a complete set of radiation data for an entire image **86** (a frame) periodically once every "frame interval" so that real-time image of a patient placed within the x-ray beam **80** may be obtained. Typical frame rates are in the order of thirty frames per second or thirty complete readouts of the CCD detector area to the computer **22** each second.

Each frame of data is stored in the memory of the computer **22** and held until after complete storage of the next frame of data. The memory of the computer **22** also holds an average frame of data which represents an historical averaging of frames of data as will now be described and which is normally used to generate the image on the video monitor **18**.

In a typical image **86**, there will be some stationary object **90** such as bone and some moving object **92** such as a surgical instrument such as a catheter. In a second image **86'** taken one frame after the image **86**, the bone **90** remains in the same place relative to the edge of the image **86** and **86'**, however the surgical instrument **92** has moved. Accordingly, some pixels **88'** show no appreciable change between images **86** and **86'**, whereas some other pixels **88"** show a significant change between images **86** and images **86'**.

Referring now to FIG. **9**, as data arrives at the computer **22**, the computer **22** executes a stored program to compare current pixels of the image **86'** to the last pixels obtained from image **86** as indicated by process block **94**. This comparison is on a pixel by pixel basis with only corresponding pixels in the images **86** and **86'** compared. The difference between the values of the pixels **88**, reflecting a difference in the amount of x-ray flux received at the CCD camera **84**, is mapped to a weight between zero and one, with greater difference between pixels **88** in these two images corresponding to larger values of this weight w. This mapping to the weighting is shown at process block **96**.

Thus pixels **88"**, whose value changes almost by the entire range of pixel values between images **86** and **86'**, receive a weighting of "one" whereas pixels **88'** which have no change between images **86** and **86'** receive a value of zero. The majority of pixels **88** being neither unchanged nor radically changed will receive a value somewhere between zero and one.

Generally, because the amount of x-ray fluence in the beam **80** is maintained at a low level to reduce the dose to the patient, the images **86** and **86'** will have appreciable noise represented as a speckling in the images **86** and **86'**. This noise, being of random character, may be reduced by averaging data for each pixel **88** over a number of frames of acquisition effectively increasing the amount of x-ray contributing to the image of that pixel.

Nevertheless, this averaging process tends to obscure motion such as exhibited by the surgical instrument **92**. Accordingly, the present invention develops an average image combining the values of the pixels acquired in each frame **86**, **86'** in which those pixels in the current image **86'** which exhibit very little change between images **86** and **86'** contribute equally to the average image, but those pixels in the current image **86'** that exhibit a great degree of change between images **86** and **86'** are given a substantially greater weight in the average image. In this process, a compromise is reached between using historical data to reduce noise and using current data so that the image accurately reflects changes. Specifically, the value of each pixel displayed in the image is computed as follows.

$$P_i=(1-w)P_{i-1}+wP_{i,t} \quad (1)$$

where P_{i-1} is a pixel in the previous average image, w is the weighting factor described above and $P_{i,t}$ is the current data obtained from the CCD camera **84**. This effective merger of the new data and the old data keyed to the change in the data is shown at process block **98**.

Image Intensifier Distortion

Referring now to FIG. **10**, an image **86"** of a rectilinear grid **100** positioned in the x-ray beam **80** will appear to have a barrel or pincushion shape caused by distortion of the image intensifier **82** and the optics of the CCD camera **84**. During a real-time use of the image **86"** by a physician, this distortion may cause confusion by the physician controlling a tool **102**. For example, tool **102** may be a straight wire shown by the dotted line, but may display an image **86'** as a curved wire whose curvature changes depending on the position of the tool **102** within the image **86**. This distortion thus may provide an obstacle to a physician attempting to accurately place the tool **102** with respect to an object within the image **86'**.

Referring now to FIG. **11**, the distortion of image **86"** also means that two equal area regions of interest **105** (equal in area with respect to the image) do not encompass equal areas of the x-ray beam **80** received by the image intensifier **82**. Accordingly, if the data from the CCD camera **84** is used for quantitative purposes, for example to deduce bone density, this distortion will cause an erroneous variation in bone density unrelated to the object being measured.

Accordingly, the present inventors have adopted a real-time digital re-mapping of radiation data from the CCD camera **84** to the image **86** to correct for any pincushion-type distortion. This remapping requires the imaging of the rectilinear grid **100** and an interpolation of the position of the radiation data received from the CCD camera **84** to new locations on the image **86"** according to that test image. By using digital processing techniques in a dedicated image processor **27**, this remapping may be done on a real-time basis with good accuracy.

Referring to FIG. **19**, there are two types of distortion, isotropic and anisotropic. Isotropic distortion is rotationally symmetric (e.g. like barrel and pin cushion distortion). Anisotropic distortion is not rotationally symmetric. Both types of distortion and rotation are so-called third order aberrations which can be written in the form:

$$Dx=r^2(Du-dv) \quad (2)$$

$$Dy=r^2(Dv+du) \quad (3)$$

where Dx and Dy are pixel shifts due to distortion; r is the distance from the correct position to the optical axis and D and d are distortion coefficients which are constant and u and v are correct pixel positions.

Referring also FIG. **2**, received image **86** may exhibit pin cushion distortion evident if an image **86** of the rectilinear grid **100** is made. The distortion is caused by the pixel shifts described above.

Equations 1 and 2 may be rewritten as third order two-dimensional polynomials, the case for equation (1) following:

$$x=(a_x+e_xv+i_xv^2+m_xv^3)+(b_x+f_xv+j_xv^2+n_xv^3)u+(c_x+g_xv+k_xv^2+o_xv^3)u^2+(d_x+h_xv+l_xv^2+p_xv^3)u^3 \quad (4)$$

In these polynomials, a_x and a_y govern the x and y translation of the image, e_x and b_y take care of scaling the output image, while e_y and b_x enable the output image to rotate. The remaining higher order terms generate perspective, sheer and higher order distortion transformations as will be understood to those of ordinary skill in the art. Thirty-two parameters are required for the two, third order polynomials. These parameters may be extracted by a program executed by the computer in an off-line (non-imaging) mode after imaging the known grid **100** and comparing the distorted image of the grid **100** to the known grid **100** to deduce the degrees of distortion.

Referring now to FIG. **19** in a first step of the correction process, the grid **100** is imaged as indicated by process block

160 to determine the exact type of distortion present and to obtain values for the coefficients a through p of the above referenced polynomial equations.

At process block **166**, these parameters may be input to the computer **22** and used at a transformation of received image **86** into image data **164** as indicated by process block **168**. For rotation of the image **164**, new parameters of the polynomials may be entered by means of hand-held remote control wand **63** shown in FIG. **1**.

The transformation process generally requires a determination of the pixel shift for each radiation pixel **163** of the input image **86** which in turn requires an evaluation of the polynomials whose coefficients have been input. A number of techniques are known to evaluate such polynomials including a forward differencing technique or other techniques known in the art. These transformations provide values of u and v for an image pixel **170** corresponding to a particular radiation pixel **163**.

After the transformation of process block **168**, the u, v locations of the radiation pixels will not necessarily be centered at a pixel location defined by the hardware of the video monitor **18** which usually spaces pixels **170** at equal distances along a Cartesian axis. Accordingly, the transformed pixels must be interpolated to actual pixel locations as indicated by process block **172**.

A number of interpolation techniques are well known including bilateral and closest neighbor interpolation, however in the preferred embodiment, a high resolution cubic spline function is used. A given value of an interpolated pixel **170** (P_{int}) is deduced from a 4×4 block of transform pixels ($P_{i,j}$) in which it is centered as follows:

$$P_{int}=f(n-2)X_1+f(n-1)X_2+f(n)X_3+f(n+1)X_4 \quad (5)$$

where:

$$X_i=f(m-2)P_{i,1}+f(m-1)P_{i,2}+f(m)P_{i,3}+f(m+1)P_{i,4} \quad (6)$$

where:

$$f(x)=(a+2)x^3+-(a+3)x^2+1 \text{ for } x\epsilon[0,1];$$

$$f(x)=ax^3+-5ax^2+8ax-4a \text{ for } x\epsilon[1,2]; \quad (7)$$

f(x) is symmetrical about zero. In the preferred embodiment a=−0.5

and where m and n are fractions indicating the displacement of the neighboring pixels $P_{i,j}$ with respect to P_{int} in the x and y directions, respectively.

At process block **180**, the transformed and interpolated image is displayed.

Noise Equalization

Referring now to FIG. **12**, the radiation data from the CCD camera **84** are mapped to the brightness of the pixels of the image **86** according to a second transformation. In the preferred embodiment, this mapping between CCD radiation data and image pixel brightness follows a nonlinear curve **103** based on the hyperbolic tangent and being asymptotically increasing to the maximum CCD pixel value. This curve is selected from a number of possibilities so that equally wide bands of image pixel brightness **104** and **106** have equal amounts of image noise. The curve **103** is further positioned to provide the maximum contrast between clinically significant tissues in the image.

Exposure Control

The noise in the image **86** is further reduced by controlling the fluence of the x-ray beam **80** as a function of the density of tissue of the patient within the beam **80**. This density is deduced from the image **86** itself produced by the CCD camera **84**. In response to the image data, a control signal is sent via the fiber optic strand within the cable **60** to the x-ray tube power supply **74** positioned adjacent to the x-ray tube **68** (shown in FIG. **5**). By positioning the x-ray tube power supply **74** near the x-ray tube **68**, extremely rapid changes in the power supplied to the x-ray tube **68** may be obtained. Distributed capacitances along high tension cables connecting the x-ray tube **68** to a stationary x-ray tube power supply are thus avoided in favor of low voltage cable **60**, and the shielding and inflexibility problems with such high tension cables are also avoided.

Automatic Technique Control

Referring now to FIGS. **13** and **14**, a determination of the proper control signal to send to the x-ray tube power supply **74** begins by analyzing the image data **86** as shown in process block **120**. The goal is to provide for proper exposure of an arbitrary object placed within the x-ray beam **80** even if it does not fill the field of view of the CCD camera **84**. For this reason, it is necessary to eliminate consideration of the data from the CCD camera **84** that form pixels in the image corresponding to x-rays that bypass the imaged object and are unattenuated ("background pixels"). These background pixels may be arbitrarily distributed in the image **86** and therefore, this identification process identifies these pixels based on their value. To do this, the computer **22** collects the values of the pixels from the CCD camera **84** in a histogram **122** where the pixels are binned according to their values to create a multiple peaked plot. The horizontal axis of the histogram **122** may for example be from 0 to 255 representing 8 bits of gray scale radiation data and the vertical axis may be a number of pixels having a particular value.

If there is a histogram value at horizontal value 255, and the maximum gray scale exposure recorded, the entire area of the histogram **122** is assumed to represent the imaged object only (no background pixels). Such a situation represents an image of raw radiation only or a high dose image of a thin object with possible clipping. In assuming that the whole histogram **122** may be used to calculate technique without removal of background pixels, a reduced exposure rate will result as will be understood from the following description and the peak classification process, to now be described, is skipped.

Otherwise, if there are no pixels with the maximum value of 225, the present invention identifies one peak **124** in the histogram **122** as background pixels indicated by process block **120** in FIG. **14**. In identifying this peak **124**, the computer **22** examines the histogram **122** from the brightest pixels (rightmost) to the darkest pixels (leftmost) assuming that the brightest pixels are more likely to be the unattenuated background pixels. The process block **120** uses several predetermined user settings as will be described below to correctly identify the peak **124**.

Once the peak **124** has been identified, the pixels associated with that peak are removed per process block **126** by thresholding or subtraction. In the thresholding process, pixels above a threshold value **138** below the peak **124** are considered to be background pixels and are omitted from an exposure rate calculation. In the subtraction method, the peak **124** itself is used as a template to identify pixels which will be removed.

At process block **128**, an exposure rate is calculated based on the values of the pixels in the remaining histogram data

and at process block **130**, an amperage and voltage value are transmitted via the cable **60** to the x-ray tube power supply and used to change the power to the x-ray tube. Generally, if the exposure rate is above a predetermined value, the amperage and voltage are adjusted to cut the x-ray emission from the x-ray tube, whereas if the exposure rate is below the predetermined value, the amperage and voltage are adjusted to boost the exposure rate to the predetermined value.

Referring now to FIGS. **13**, **14** and **15**, the process of identifying background pixels will be explained in more detail. Process block **120** includes as a first step, an identification of a right most peak **124** in the histogram **122** (shown in FIG. **13**) as indicated by subprocess block **132**.

At succeeding subprocess block **134**, this right most peak **124** is compared against three empirically derived parameters indicated in the following Table 1:

TABLE 1

Minimum Slope Range (MSR)	Minimum necessary pixel range for which the slope of the peak must be monitonically increasing.
Histogram Noise Level (HNL)	Minimum height of the maximum value of the peak.
Maximum Raw Radiation Width (MRRW)	Maximum width of the detected peak with respect to the width of the entire histogram.

Specifically at subprocess block **134**, each identified peak **124** is tested against the three parameters indicated in Table 1. In the description in Table 1, "width" refers to the horizontal axis of the histogram **122** and hence a range of pixel values, whereas "height" refers to a frequency of occurrence for pixels within that range, i.e., the vertical axis of the histogram **122**.

These first two tests, MSR and HNL, are intended to prevent noise peaks and peaks caused by bad imaging elements in the CCD camera **84** or quantization of the video signal in the A to D conversion from being interpreted as background pixels.

Peaks **124** with a suitable stretch of monotonically increasing slope **131** (shown in FIG. **13**) according to the MSR value and that surpass the histogram noise level HNL **133** are evaluated against the MRRW parameter. This third evaluation compares the width **135** of the histogram **122** against the width of the entire histogram **122**. The MRRW value is intended to detect situations where the imaged object completely fills the imaging field and hence there are no unattenuated x-ray beams or background pixels being detected. A valid peak **124** will normally have a width **135** more than 33% of the total width of the histogram **122**.

At decision block **136** if the peak **124** passes the above tests, the program proceeds to process block **126** as indicated in FIG. **14**. Otherwise, the program branches back to process block **132** and the next peak to the left is examined against the tests of process block **134** until a passing peak is found or no peak is found. If no peak is found, it is assumed that there are no background pixels and a raw exposure value is calculated from all pixels as described above.

Assuming that a peak **124** passes the tests of Table 1, then at process block **126** background pixels identified by the peak **124** selected at process block **120** are eliminated.

In a first method of eliminating background pixels indicated at FIG. **16**, a magnitude threshold **138** within the histogram **122** is identified. Pixels having values above this threshold will be ignored for the purpose of selecting an exposure technique. The threshold **138** is established by identifyng the center **140** of the peak **124** (its maximum value) and subtracting from the value of the center a value s being the distance between the start of the peak **124** as one moves leftward and the maximum **140**. The area under the histogram **122** for values lower than the threshold **138** is computed to deduce a raw exposure value which will be used as described below.

In a second embodiment, the shape of the histogram peak **124** from the start of the peak as one moves leftward to its maximum **140** is reflected about a vertical line passing through the maximum **140** and subtracted from the histogram peak **124** to the left of the vertical line. This approach assumes that the peak **124** of the background pixels is symmetrical and thus this method better accommodates some overlap between the object pixels and the background pixels in the histogram **122**. Again, the remaining pixels of the histogram **122** are summed (by integration of the area under the histogram **122** minus the area of the peak **124** as generated by the reflection) to provide a raw exposure value.

Referring now to FIG. **18**, the raw exposure value is transformed by the known transfer characteristics of the CCD camera (relating actual x-ray dose to pixel value) to produce a calculated current exposure rate as indicated at process block **144**.

Referring to process block **146**, the current exposure rate is next compared to a reference exposure rate, in the preferred embodiment being 1.0 mR per frame, however this value may be refined after further clinical testing. If at process block **148**, the current exposure rate is within a "half fine-tune range" of the reference exposure rate, then the program proceeds to process block **150**, a fine tuning process block, and the amperage provided to the x-ray tube are adjusted in accordance to the disparity between the amperage and reference exposure rate. That is, if the current exposure is greater than the reference exposure rate, the amperage to the x-ray tube is reduced. The new value of amperage is compared against a predetermined range of amperage values (maximum beam current and minimum beam current values) so that the amperage value may never vary outside of this range.

If at decision block **148**, the current exposure rate is outside of the half fine tune range established at decision block **148**, a more substantial adjustment process is undertaken. Generally, the exposure provided by an x-ray system will follow the following equation:

$$X \approx s \cdot mA \cdot kVp^{n}. \tag{8}$$

where:

s is seconds,

mA is the amperage provided to the x-ray tube,

kVp is the voltage provided to the x-ray tube, and

n is a power factor dependent on the geometry of the machine and the particular kind of object being imaged.

Generally, the value of n will not be known in advance. Accordingly in the more substantial correction process, n is deduced by obtaining two different exposures for equal predetermined intervals with different kVp values so that the value of n may be deduced.

At decision block **152**, it is determined whether a first or second reference exposure is to be obtained. If the first reference exposure was just obtained, the program proceeds to process block **154** and a new value of kVp is determined for a second exposure. In this case, the first exposure used will be that which was employed to produce the histogram **122** as previously described.

If the comparison of process block **148** indicated that the exposure rate was too high, a lower kVp value is selected; and conversely, if the exposure at process block **148** indicated the exposure was too low, an increased value of kVp is provided. The new kVp value for the second exposure must be within a predetermined range of kVp values established by the user. Mathematically, the kVp value selected may be described as:

$$kVp_2=kVp_1+a(dkVp) \tag{9}$$

where a is a step factor and

dkVp is a minimum practical change in tube voltage.

Two preferred means of selecting may be used: one providing linear and one providing logarithmic scaling. Such scaling techniques are well understood to those of ordinary skill in the art.

If at decision block **152**, a second frame has already been taken with the new voltage value, then the program proceeds to process block **156** and the value of n in equation (9) is calculated. If the value of amperage is held constant between the first and second frame, the value of n may be determined according to the following equation:

$$n = \log\frac{X_2}{X_1} \Big/ \log\frac{kVp_2}{kVp_1} \tag{10}$$

where X_1 and X_2 are the measured exposure rates at the first and second frames, respectively and kVp_1 and kVp_2 are the two x-ray tube voltages during the first and second frames.

At process block **158**, this value of 'n' is checked against threshold values intended to detect whether an erroneous value of n has been produced as a result of 'clipping' in the radiation data used to calculate exposure. As is understood in the art, clipping occurs when an increased dose of an element of the CCD camera produces no increase in the camera's output.

At decision block **158**, if the value of n calculated at process block **156** is greater than or equal to one, it is assumed to be valid and the program proceeds to process block **160** where kVp and mA are adjusted by setting mA equal to a maximum reference value and calculating kVp according to the following equation:

$$kVp_{new} = kVp_2\left(\frac{X_{ref}mA_2}{X_2mA_{ref}}\right)^{1/n} \tag{11}$$

where kVp_{new} and mA_{new} are the settings for the next frame to be shot.

If the resulting kVp value conflicts with the minimum system, kVp, kVp is set to the minimum system value and mA is calculated according to the following equation using the mA and kVp value of the second frame.

$$mA_{new} = mA_2\frac{X_{ref}}{X_2}\left(\frac{kVp_2}{kVp_{\min}}\right)^n \tag{12}$$

If the value of n in decision block **158** is less than one, then at process block **162**, n is tested to see if it is less than zero. This value of n is realized when the exposure rate of the second frame changes in the opposite direction of the tube voltage. This suggests a clipped histogram and therefore the program branches back to process block **154** to obtain a new second frame. This condition may also arrive from object motion between the first and second frame.

On the other hand, if at decision block **162**, n is not less than zero (e.g. n is between zero and 1), the program proceeds to process block **166**. Here it is assumed that because the sensitivity of the exposure rate on change in kVp is low, there may be some partial clipping. New values of kVp and mA are then computed and used with the previous second frame values to calculate a new n as follows. Generally, if kVp and mA are high, they are both lowered and if kVp and mA are low, they are both raised.

Scatter Reduction

Referring now to FIG. **1**, the image produced by the present invention may be used for quantitative analysis including, for example, that of making a bone density measurement. It is known to make bone density analyses from x-ray images through the use of dual energy techniques in which the voltage across the x-ray tube is changed or a filter is periodically placed within the x-ray beam to change the spectrum of the x-ray energy between two images. The two images may be mathematically processed to yield information about different basis materials within the image object (e.g. bone and soft tissue). For these quantitative measurements, it is desirable to eliminate the effect of scatter.

Referring now to FIG. **23** in imaging a patient's spine **200**, for example, x-rays **202** are directed from an x-ray source **201** through the patient **199** to pass through soft tissue **204** surrounding a spine **200**. Certain of the x-rays **202** are blocked by the spine **200** and others pass through the spine **200** to be recorded at the image intensifier **206**. An attenuation image **208** measured by an image intensifier measures those x-rays passing through the patient **109**.

A portion **210** of the attenuation image directly beneath the spine **200** records not only those x-rays **202** passing through the spine **200** and the soft tissue **204** above and below it, but also scattered x-rays **212** directed, for example, through soft tissue **204** to the side of the spine **200** but then scattered by the soft tissue to proceed at an angle to the portion **210** of the attenuation image **208** beneath the spine **200**. Because the scattered x-rays **212** do not carry information about the attenuation of the spine **200**, they are desirably removed from the image **208** prior to its use in quantitative measurement.

For this purpose, the present invention uses an occluder **214** being an x-ray transparent plate such as may be constructed of Plexiglas and incorporating into its body, a plurality of x-ray blocking lead pins **216**. Preferably these pins are placed so as to project images **218** onto the image **208** received by the image intensifier **206** in positions outside an image **220** of the spine **200**. Generally therefore, the pins **216** are placed at the periphery of the occluder **214**. The pins **216** are sized so as to substantially block all direct x-rays from passing through them but so that their images **218** include a significant portion of scattered x-rays **212**.

Referring now to FIG. **22** at a first step of a scatter reduction operation with the occluder **214** of FIG. **21**, an image is acquired of the imaged object, for example, the spine **200** and its surrounding soft tissue **204** (not shown in FIG. **21**) including the images **218** of the pins **216**. This acquisition is indicated by process block **221** of FIG. **22**.

The pins **216** are held in predetermined locations with respect to the image **208** so that their images **218** may be readily and automatically identified. Preferably the pins **216** are placed at the interstices of a Cartesian grid, however, other regular patterns may be chosen. The image **208** may be corrected for pincushion type distortion, as described above,

so that the locations of the pins **216** may be readily located in the image based on their known positions in the occluder **214**.

At each pin image **218**, a value **222** indicating the magnitude of the received x-rays, shown in FIG. **23**, may be ascertained. This value **222** measures the scatter received in the vicinity of image **218** caused generally by the effect of the soft tissue **204** and possible secondary scatter effects in the image intensifier **206**. Values **222** are recorded, as indicated by process block **224**, for each pin image **218**. From these values, a set of normalizing points are established.

The image **208** is then used to derive a scatter map. Referring to FIG. **23**, generally the amount of scatter at a given point will be a function of how many x-ray photons are received at points adjacent to the given point. For example, comparing the image **208** to a theoretical scatterless image **228** generally in an attenuated region **230** of the image **208** (e.g., under the spine **200**), scatter will increase the apparent value in the image **208** as a result of radiation from nearby low attenuation regions scattering into the high attenuation region **230**. Conversely the apparent value at a low attenuation region **232** will be decreased because of the scatter into the high attenuation region.

A map of the scattered radiation may thus be modeled by "blurring" the image **208**. This blurring can be accomplished by a low pass filtering of the image **208**, i.e., convolving the image **208** with a convolution kernel having rectangular dimensions corresponding to the desired low pass frequency cut off. The effect is an averaging of the image **208** producing scatter map **234**.

The image used to produce the scatter map **234** is an attenuation image **208** obtained from the patient **199** without the occluder **214** in place, or may be an image **208** including the images **218** of the pins **216** but with the latter images **218** removed based on knowledge of their location. This removal of images **218** may substitute values of the image **208** at points **239** on either side of the images **218**. The process of driving the scatter map from the image is indicated by process block **235** of FIG. **24**.

Next as indicated by process block **237**, the scatter map **234** is fit to the normalizing points **222** previously determined at process block **224**.

Referring to FIG. **24**, the scatter map **234** is thus normalized so that the portions **238** of the scatter map **236** located near the places where the images **218** would fall are given values **222** as determined at process block **224**. This involves a simple shifting up or down of the scatter map **236** and may employ a "least square" fit to shift the scatter map **236** to multiple values **222** obtained from each pin **216**. As adjusted, the scatter map **236** is then subtracted from the image **208** to eliminate or reduce the scatter in that image as indicated by process block **239**.

The effect of subtracting a low pass filtered or blurred image properly normalized to actual scatter is to sharpen up the image **208** but also to preserve its quantitative accuracy. Thus the present invention differs from prior art scatter reduction techniques in that it both addresses the variation in scatter across the image caused by attenuation of x-rays by the imaged object but also incorporates accurate measurements of scatter in certain portions of the image.

Densitometer Adapter

Referring now to FIG. **25**, a mobile fluoroscopy machine **310** suitable for use with the present invention is similar to that which has been described above with respect to FIG. **1** with exceptions that will be apparent from context.

The mobile fluoroscopy machine **310** includes a mobile cart **312** supporting a computer **314** and monitor and keyboard **317** for receiving and processing digital x-ray image data. The cart **312** supports on one side an articulating arm assembly **316** terminating in a rotatable C-arm **318**. The C-arm supports, at the ends of the C, an image intensifier **320** and an x-ray source **322** opposed along an axis **324** so that the x-ray source **322** projects a cone-beam of x-ray radiation toward the image intensifier **320** along axis **324**.

The articulating arm assembly **316** is connected to the C-arm **318** through one or more pivotal links **327** so that the axis **324** may be positioned to be horizontal approximately two feet above the floor to rest upon or be supported against the upper end of a supporting pedestal **326** or may be attached to the cart **312**. Referring also to FIG. **26**, the pedestal **326** includes a hemicylindrically concave cradle **328** at its upper surface to receive a lower portion of the cylindrical image intensifier **320** when the C-arm is so positioned to rest against the pedestal **326**.

The pedestal **326** also provides on its upper surface a channel **330** extending across the axis **324** between the image intensifier **320** and the x-ray source **322** when the latter are positioned on the pedestal **326**. The channel **330** may receive a limb positioner **332** such as may be adapted to support a patient's foot or arm across the axis **324** for densiometric measurement. The pedestal **326** may be weighted so as to provide a stable surface for support of the x-ray source **322** and image intensifier **320** and to provide adequate support for the patient's limb. The height of the pedestal **326** is selected to be suitable for either arm or foot imaging.

Referring now to FIGS. **27** and **30**, the channel **330**, extending substantially perpendicularly to axis **324** and has a horizontal bottom surface **333** pierced by two vertically extending guide holes **334** which may be used to receive and position corresponding pins **337** on one of two limb positioners **332**. A foot positioner **336**, as shown in FIG. **26**, provides a padded calf support plate **338** fitting adjacent to the bottom surface **333** and an upwardly extending sole support **340** forming an obtuse angle with respect to the calf support plate **338**. A cushion **342** on the calf support plate **338** may be adjusted so as to allow the patient's leg to extend upward somewhat from vertical for comfort. Gussets **344** span the angle between the sole plate **340** and calf support plate **338** to fix them in relative position but include apertures **346** to allow for the free passage of x-rays through a portion along axis **324** where the os calcis of the heal will be located.

When positioned within the channel **330**, the foot positioner **336** is also supported by upwardly extending channel sidewalls **348** which serve further to provide an alignment surface for the imaging face of the image intensifier **320** or other detector array and on the other side, an alignment surface for an emitting face of the x-ray source **322**. Channel sidewalls **348** are generally radio translucent so as to permit the passage of x-rays therethrough, but may include: calibration materials such as are well known in the art for calibrating dual energy devices, antiscatter grids also well known in the art, or occluders for evaluating scatter as have been described above or in the parent applications hereby incorporated by reference. removed and a palm support **352** is inserted by means of pin **337** in one of the holes **334** so as to locate a user's arm resting against the bottom surface **333** with the user's palm against the palm support **352** such that the bones of the forearm are placed along the axis **324** for imaging.

Referring to FIGS. **28** and **29**, the hemispherical support cradle **328** may include three radially inwardly extending

ribs **354** attached by means of screws or the like to be replaceable. Two of the ribs **354** are positioned in a horizontal plane to substantially bisect the image intensifier **320** when it is placed within the cradle **328**. The third rib **354** is positioned at the bottom of the cradle **328** and is opposed by a rotating locking collar **358** which may be used to further secure the image intensifier **320** within the cradle **328**. The front edge of the image intensifier is abutted against the upright face of the dividing barrier so as to precisely locate it along axis **324**. The inner edges of these ribs **354** define an inner radius **356** of lesser diameter than the cradle **328** that by proper design of the ribs **354** may be adjusted to conform to the outer surface of a particular image intensifier **320**.

Referring now again to FIG. **30**, some fluoroscopy equipment will not permit digital imaging or the necessary dual energy control needed for densitometry. Accordingly, an independent detector array **360** may be placed within the cradle **328** in lieu of the image intensifier **320**. This detector array **360** may be a pair of stimulable phosphor plates as are understood in the art with intermediate filtering so as to provide dual energy readings with a polychromatic x-ray source. In this way a switching of voltage on the x-ray source **322**, as described above, can be avoided. Alternatively, the detector array **360** may be a large area solid state detector or scanning detector assembly such as are understood in the art including those constructed of amorphous silicon and thin film transistor technology or those employing active pixel technology in which C-MOS integrated circuit fabrication techniques are employed. These detectors may be used with a switched x-ray source **322** to provide dual energy imaging or may be used in a stacked configuration with intermediate filtering so as to provide separate energy measurements, or may be used in a side-by-side configuration with interleaved detector elements filtered so as to be selectively sensitive to different energies.

In the preferred embodiment, and as shown in FIG. **31**, the independent detector array **360** is a "pancake" image intensifier **361**, suitably small so as to fit within the space between a conventional image intensifier **320** and the x-ray source **322**. Referring to both FIG. **30** and **31**, the pancake image intensifier **361** includes a vacuum bowl **362** having a planar front surface **364** for receiving x-rays **366** (normally through the channel sidewalls **348** of the stand **326**).

According to conventional design, the x-rays **366** pass through the front surface **364** of the vacuum bowl **362** to strike a target material **368** to eject electrons **370** into the volume of the bowl **362**. Focusing electrodes **372** direct the electrons to a phosphor **374** where an image is formed to be received by imaging array **375** such as a CCD array or camera. The image area of the phosphor **374** is much smaller than the front surface **364** so as to reduce the image size to one compatible with the camera. In the present invention the distance B between the target **368** and the imaging array **375** (including any optical path through one or more focusing lenses) is less than or equal to the radial dimension. A of the front surface **364** gives the pancake image intensifier **361** an extremely short form factor suitable for practice with the present invention.

Hitherto, such form factors were avoided because they are known to result in severe distortion of the image formed on the phosphor **374**. This distortion is accommodated in the present invention by means of digital image processing in computer **314** which receives digitized pixel data from scanning electronics **378** connected to the imaging array **375** and corrects it according to the correction process described above with respect to the pin cushion correction. Accordingly, the addition of digital signal processing allows for production of pancake image intensifier **361** in which the separation of the imaging optics from the front of the image intensifier is much reduced.

The above adapter may be modified to use in femur imaging. In this case the pedestal **326** may be eliminated in favor of a positioner (not shown) attached to the image intensifier **320** or x-ray source **322** directly. In the former case, the positioner may provide for a fixed air gap between the patient and the image intensifier **320** to reduce received scatter. So as to allow free manipulation of the C-arm **318**, the positioner may be a lightweight plastic radiolucent material and may optionally include a calibration system such as a flip in phantom for calibration of the dual energy readings and occluders for scatter correction as has been described above. Collimation and/or a separate solid state dual energy image detectors may also be held by the positioner whose outer surface may guide the positioning of the C-arm **318** to the necessary orientation which need not be horizontal but may be vertical for fore arm measurements or the like. For femur measurements, the patient may stand and the C-arm **318** manipulated appropriately as guided by the positioner.

Referring now to FIGS. **31** and **32**, computer **314** includes a processor **380** and memory **382**, the latter of which receives raw image data in the form of pixels having spatial locations and brightness values forming images **384**. Memory **382** also includes a processing program **386** providing a general interface and control of the operation of the fluoroscopy machine **310** and a processing of images **384** so as to provide a quantitative measure of bone isolated from soft tissue.

The processing program **386** can be simply loaded into the computer **314** for the fluoroscopy machine **310** when the pedestal **326** is to be employed with a fluoroscopy machine **310** providing digital imaging and x-ray voltage control. If an independent detector array **360** is required, the program **386** may be executed on a computer **314** associated with that independent detector array **360**.

At a first step in the program **386**, indicated by process block **388**, the operator of the fluoroscopy machine **310**, having indicated a desire to perform densitometry and having positioned the C-arm in the pedestal **326**, enters patient data that will be used to identify the image **384** to be collected.

At succeeding process block **390**, data is collected for three distinct images **384** with: 1) no x-ray exposure, 2) high energy x-ray exposure, and 3) low energy x-ray exposure. Each of the exposures is preserved as a separate image file in the memory of the computer **314**. The first exposure is used for correction routines to be described; the latter two exposures are used to deduce bone density according to methods well known in the art in which variations in high energy and low energy absorption are used to deduce the Compton scattering and atomic number of the material lying between the x-ray source **322** and the image intensifier **320**. As is understood in the art, these two measurements allow the amount of bone as opposed to soft tissue located in that image region to be accurately measured. The data is acquired directly from the independent detector array **360** or in the event that stimulable plates are used, a reader may be attached to the computer **314** so as to acquire the necessary pixel data of an image **384**. In the same way a conventional photographic film/filter plate arrangement may be used.

At next process block **393**, each of these images is corrected for non-linearity of the detector such as may be

determined empirically at an earlier time by testing the detector according to methods well known in the art, and which is a function of the detector and the technology used by the detector. Generally the testing exposes the detector to different fluences of x-rays and measures the output of the detector and the correction is intended to ensure that, for example, a doubling of fluence results in a doubling of detector output after correction. The correction is generally simply a scaling of each of the images by a factor that is a function of the pixel value for each pixel and possibly the location of the pixel.

At process block **395**, noise related to the particular line of the detector is removed. Referring to FIG. **34**, the imaging array **375** provides a matrix of detector elements **392** arranged in rows and columns. Normally, either rows or columns are ganged together to be read out by dedicated read out electronics **391** spanning a particular row or column. The read out electronics introduces noise which is imposed upon each detector element **392** of that row and which is thus line correlated, that is, more highly correlated with other detector elements **392** of the line than detector elements **392** of different lines. To eliminate line correlated noise, one detector element **392** in each line is blocked by a lead mask **394** so as to be shielded from x-rays. A pixel value **396** from this blocked detector element **392** will provide a value that varies according to the line noise thus a line correlated noise value **398** may be deduced and subtracted from the pixel values **400** of the other detector elements **392** in the line.

Referring again to FIG. **32**, at a succeeding process block **402**, veiling glare is removed and the field is flattened. This former correction attempts to eliminate blurring of the image such as may be caused by scatter or similar effects within the imaging array **375**. Glare refers generally to a reading that would be obtained under detector elements **392** that were wholly shadowed by an occluding absorber on the surface of the array **375**. The glare is a function of the detector technology and is reduced by a deconvolution process based on an empirically derived deconvolution kernel according to a number of techniques well known in the art.

Also at process block **402** the field is flattened which is to say the gain variation of the detector elements **392** are normalized according to an empirically derived normalization map determined at the factory by exposing the detector to a uniform x-ray elimination and noting variation and intensities reported in the pixel values **400**. At this time, dark currents from the detector elements **392** may also be eliminated as determined from the no-exposure x-ray image taken at process block **390**.

Referring now to process block **404**, a dynamic scatter correction may be employed as has been previously described with respect to FIGS. **21–23**. Alternatively referring also to FIG. **33**, a dynamic scatter correction may be employed in which the data of the image **384** is analyzed so as to create a histogram **406** of pixel values **400** for the entire image. The histogram may be divided into regions **408** (five equal regions in the preferred embodiment) corresponding roughly x-ray paths through: 1) air-only, 2) thin tissue, 3) thick tissue only, 4) thin bone and, and 5) thick-bone. Each of these materials will exhibit a different scattering and hence a different empirically derived scatter kernel **410** may be assigned to each region **408** with generally the lower density regions having narrower kernels commensurate with less scatter.

The selected scatter kernel **410** may be scaled by the pixel value of the image **384** on a pixel by pixel basis and that kernel, so scaled, applied to a deconvolver **412** used to deconvolve the image **384** to produce a deconvolved image **414**. A number of techniques of deconvolution are well known in the art using a fixed scatter kernel and these same techniques may be used with the variable scatter kernel **410** described here. During deconvolution the kernel **410** will be sequentially applied to a set of adjacent pixel values determined by the width of the kernel. The center pixel value at any step of the deconvolution will be used to scale the kernel and to identify the region of the histogram for the purpose of selecting the kernel **410**. In an alternative embodiment, the kernel may be fixed and simply scaled by the value of the centermost pixel during de-convolution.

Referring again to FIG. **32**, at process block **416**, the images **384** are log corrected reflecting the fact that attenuation is exponentially related to thickness. The images are now related to thickness, a dimension which will be important in the ultimate bone-density determination.

At following process block **418**, speckle may be identified for certain x-ray detectors **360** that are subject to extremely high readout values caused by noise which is possibly related to direct x-ray irradiation of the detector element. Speckle is identified by a simple thresholding process.

At next process block **420**, path length correction may be performed based on the geometry of the particular C-arm such as may vary path length and magnification across the image as is well understood in the art.

Similarly at succeeding process block **422**, beam hardening, the well known effect of a spectral shift in a polyenergetic x-ray beam as it passes through different thicknesses of material, and a Heel effect correction may be made, the Heel effect correction referring to a variation in the spectrum of an x-ray beam as a function of its angle in the cone of x-ray beams. Both of the corrections are known in the art, but must be employed in the present invention in order to provide suitable quantitative accuracy for densitometry.

At process block **424**, the identified speckle of process block **418** is corrected by eliminating these identified pixels from subsequent calculation or by replacing them with a local average value.

The entire image may then be averaged or low-passed filtered at process block **426** so as to further reduce noise and to eliminate unneeded resolution.

The images are then processed according to well understood techniques to produce a bone mineral density value at process block **428**. This bone mineral density value indicates the amount of bone material at each pixel of the image largely independent of surrounding soft tissue. The pixel image may be analyzed in a number of methods but most simply, as indicated by process block **430**, by defining either automatically or manually a desired region of interest within the image and making a measurement of total bone density within that region. Automated techniques may look for a local maximum or minimum of bone density or may use image recognition type techniques to locate reproducibly a particular region of the forearm or os calcis. Morphometric analysis may be applied to the image to detect bone fracture and other techniques such as texture analysis may be performed according to methods well known in the art. The results of the analyses and images so processed may be displayed by the computer **314**.

It is thus envisioned that the present invention is subject to many modifications which will become apparent to those of ordinary skill in the art. Accordingly, it is intended that the present invention not be limited to the particular embodi-

ment illustrated herein, but embraces all such modified forms thereof as come within the scope of the following claim.

We claim:

1. A positioner for a fluoroscopy machine of a type having a radiation source and detector separated along a beam axis and mounted on an articulated arm, the positioner comprising:

a weighted base supporting the positioner upon a floor;

a pedestal extending upward from the base to provide receiving supports for at least one of the radiation source and detector so that when the at least one of the radiation source and detector is received by the receiving supports, the beam axis is in predetermined orientation with respect to the top of the pedestal; and

a limb positioner attached to the pedestal between the receiving supports so that a patient's limb held by the limb positioner is intersected by the beam axis.

2. The positioner as recited in claim **1** wherein the limb positioner is removable and is sized to receive the patent's limb, wherein the limb is an arm, a hand, a leg or a foot.

3. The positioner as recited in claim **1** wherein the limb positioner is a vertically extending palm support.

4. The positioner as recited in claim **3** wherein the palm support is attached to a mounting pin sized and positioned to fit within a guide bore in the pedestal.

5. The positioner as recited in claim **4** wherein the palm support is removable.

6. The positioner as recited in claim **1** wherein the limb positioner is a foot cradle having:

a calf support plate adjacent to the top of the pedestal having at least one mounting pin depending downward sized and positioned to fit within a guide bore in the pedestal;

a sole support plate joined to the calf support plate to define an obtuse angle; and

side gussets spanning the calf support plate and the sole support plate, the gussets having apertures positioned to be at the beam axis when the foot cradle is mounted to the pedestal.

7. The positioner as recited in claim **6** wherein the foot cradle includes padding material at top surfaces of the calf support plates.

8. The positioner as recited in claim **6** wherein the foot cradle is removable.

9. The positioner as recited in claim **1** including a calibration material attached to the pedestal within the beam axis.

10. The positioner as recited in claim **1** including an anti-scatter grid attached to the pedestal within the beam axis.

11. The positioner as recited in claim **1** including an occlude attached to the pedestal within the beam axis.

12. The positioner as recited in claim **1** wherein the receiving supports are disposed axially along a radius of a cavity, the receiving supports extending into the cavity to define a radius of lesser diameter than the cavity according to the size of the radiation detector.

13. The positioner as recited in claim **1** further comprising an index guide adjacent to the limb positioner for properly aligning the radiation detector with the limb positioner on the pedestal.

14. The positioner as recited in claim **1**, further comprising:

an independent detector array located along the beam axis between the limb positioner and the radiation detector when the radiation detector is disposed in the receiving supports, the detector array producing attenuated dual energy signals; and

a processor receiving the attenuated dual energy signals and calculating bone density measurements.

15. The positioner as recited in claim **14** wherein the detector array is a set of stimulable phosphor plates.

16. The positioner as recited in claim **14** wherein the detector array is solid state detector.

17. The positioner as recited in claim **14** wherein the detector array is a stacked linear array scanning detector.

* * * * *

UNITED STATES PATENT AND TRADEMARK OFFICE

CERTIFICATE OF CORRECTION

PATENT NO. : 6,315,445 B1
DATED : November 13, 2001
INVENTOR(S) : Richard B. Mazess et al.

It is certified that error appears in the above-identified patent and that said Letters Patent is hereby corrected as shown below:

Column 16,
Line 60, after "by reference.", insert -- Referring to FIGS. 27 and 28, for forearm imaging, the foot positioner 336 is --.

Signed and Sealed this

Twenty-fourth Day of September, 2002

Attest:

Attesting Officer

JAMES E. ROGAN
Director of the United States Patent and Trademark Office